MRP5 nitration by NO-releasing gemcitabine encapsulated in liposomes confers sensitivity in chemoresistant pancreatic adenocarcinoma cells

MRP5 nitration by NO-releasing gemcitabine encapsulated in liposomes confers sensitivity in chemoresistant pancreatic adenocarcinoma cells

Francesca Masetto[1], Konstantin Chegaev[2], Elena Gazzano[3], Nidula Mullappilly[1], Barbara Rolando[2], Silvia Arpicco[2#], Roberta Fruttero[2#], Chiara Riganti[3#*], Massimo Donadelli[1#*]

[1]*Department of Neurosciences, Biomedicine and Movement Sciences, University of Verona, Italy;*

[2]*Department of Drug Science and Technology, University of Turin, Italy*

[3]*Department of Oncology, University of Turin, Italy*

[#] these authors contributed equally to the work and share last authorship

***Corresponding authors:**

-Massimo Donadelli, PhD, Department of Neurosciences, Biomedicine and Movement Sciences, Section of Biochemistry, University of Verona, Italy. Strada Le Grazie 8, 37134 Verona, Italy. Phone: +39 045 8027281; fax: +39 045 8027170; e-mail: massimo.donadelli@univr.it

-Chiara Riganti, PhD, Department of Oncology, University of Torino, via Santena 5/bis, 10126 Turin, Italy. Phone: +39 011 6705857; fax: +39 011 6705845; e-mail: chiara.riganti@unito.it

Running title: NO-GEM inhibits pancreatic cancer cell growth

Keywords: nitric oxide; gemcitabine; pancreatic cancer; chemoresistance; MDR; drug delivery

ABSTRACT

Pancreatic ductal adenocarcinoma (PDAC) is a therapy recalcitrant disease characterized by the aberrations in multiple genes that drive pathogenesis and drug chemoresistance. In this study, we synthesize a library of seven novel nitric oxide-releasing gemcitabine prodrugs (NO-GEMs) in order to improve the effectiveness of GEM by exploiting the therapeutic effects of NO. Among these NO-GEM prodrugs we select **5b** as the most effective compound in GEM-resistant PDAC cells. After its encapsulation in liposomes (**Lipo 5b**) for drug delivery the intracellular NO level increases and nitration associated to activity inhibition of the multidrug resistance associated protein 5 (MRP5; ABCC5) occurs. This results in GEM intracellular accumulation and enhanced apoptotic cell death in GEM-resistant PDAC cells, which express MRP5 at higher levels than GEM-sensitive cells. Our results support the development of a new anti-tumoral strategy to efficiently affect GEM-resistant PDAC cells based on the usage of NO-GEM prodrugs.

INTRODUCTION

Pancreatic ductal adenocarcinoma (PDAC) represents the 90% of all diagnosed pancreatic cancers and is one of the most lethal solid cancer.[1] The mortality rate is almost equal to the incidence, resulting in an average survival corresponding to less than 7% at 5 years after diagnosis.[2] Chemotherapy with gemcitabine (2',2'-difluorodeoxycytidine; GEM) remains a cornerstone of PDAC treatment in all stages of the disease. It is a deoxycytidine analogue that needs to be activated by deoxycytidine kinase (dCK) to its monophosphate and subsequently to its triphosphate dFdCTP, which is incorporated into both RNA and DNA, leading to DNA damage. However, the clinical response rate of GEM treatment is generally limited by the development of chemoresistance mechanisms affecting its intracellular activation, as well as by low expression of influx proteins or overexpression of multiple drug resistance (MDR) efflux proteins, including multidrug resistance-associated proteins (MRPs) that decrease the intracellular concentration of the drug by pumping it outside the cells.[3, 4] In particular, the MRP5 isoform, encoded by the *ABCC5* gene, is described as a prominent protein for the efflux of GEM in PDAC cells[5, 6]. Multiple tumor cell-intrinsic and extrinsic mechanisms are implicated in PDAC resistance to GEM. Among the intrinsic mechanisms, the defective influx of the drug via nucleoside transporters, the defective activation via deoxycytidine kinase, the increased expression of the deoxyribonucleotide synthesizing enzyme ribonuleotide reductase all induce a genetic or acquired resistance to GEM. The prevalence of epithelial mesenchymal transition, the abundance of pancreatic stellate cells and fibroblast in the tumor stroma also make PDAC more chemoresistant.[7] It is noteworthy however that MRP5 expression level is significantly higher in PDAC tissue compared to normal pancreatic tissue[8], leading to hypothesize an active role for MRP5 in reducing GEM efficacy, by limiting the intracellular concentration of the drug and consequently its cytotoxicity.

Nitric oxide (NO) is a small free radical molecule with several physio-pathological roles in human cells.[9] Indeed, NO can promote the transient S-nitrosylation of redox-sensitive cysteines[10] or

react with superoxide ions ($O_2^{-\cdot}$) to produce peroxynitrite ($ONOO^-$), that induce a stable tyrosine nitration of proteins[11]. Nitration is involved in multiple biological processes, including signal transduction, protein degradation, energy metabolism, mitochondrial dysfunction, enzyme inactivation, immunogenic response, apoptosis, and cell death[12]. In cancers, micromolar concentrations of NO can act as an antitumor and antimetastatic agent, stimulating apoptosis and enhancing the reaction of host immune system against the tumor. Moreover, a strong relationship emerged between this molecule and the mechanism of resistance to cancer chemotherapy. Indeed, it has been demonstrated that NO can revert resistance to doxorubicin in colon cancer cells by inhibiting efflux drug-related pumps through direct tyrosine nitration[13].

In the present study, we aimed to synthetize new nitric oxide-releasing GEM pro-drugs (NO-GEMs) adding NO-donor moieties to GEM by an appropriate linker. We tested the effect of the new pro-drugs in both GEM-resistant (GEM-R) and GEM-sensitive (GEM-S) PDAC cell models and we further investigated the associated mechanisms induced by NO-GEM pro-drugs as compared to the treatment with the standard GEM molecule.

EXPERIMENTAL SECTION

Drug and reagents

Gemcitabine (2',2'-difluoro-2'-deoxycytidine; GEM) was provided by Accord Healthcare (Milan, Italy) and solubilized in dimethylsulfoxide (DMSO) (Invitrogen, Thermo Fisher) to a final concentration of 10 mM; the solution has been aliquoted and stored at -20°C. NO-donors NONOate (diethylamine NONOate diethylammonium salt) and SNAP (S-nitroso-N-acetyl-DL-penicillamine) were provided by Sigma-Aldrich (Milan, Italy), stored at -80°C or -20°C, respectively. They were freshly solubilized in H_2O for each experiment.

Synthesis of novel NO-GEM pro-drugs

Chemistry. ^{1}H and ^{13}C NMR spectra were recorded at room temperature on a JEOL ECZ-R 600 at 600 MHz and 150 MHz, or on a BrukerAvance 300, at 300 and 75 MHz, respectively, using SiMe4 as internal standard. Chemical shifts (δ) are given in parts per million (ppm) and the coupling constants (*J*) in Hertz (Hz). The following abbreviations were used to designate the multiplicities: *s* = singlet, *d* = doublet, *dd* = doublet of doublet, *t* = triplet, *q* = quartet, *qi* = quintet, *m* = multiplet, *bs* = broad singlet. ESI spectra were recorded on a Micromass Quattro API micro (Waters Corporation, Milford, MA, USA) mass spectrometer. Data were processed using a MassLynxSystem (Waters). Final compound purity was determined by HPLC analysis on Merck LiChrospher C18 endcapped column (250 x 4.6 mm ID, 5 μm) using CH_3CN 0.1% trifluoroacetic acid (TFA)/H_2O 0.1% TFA as eluent. HPLC retention time (t_R) was obtained at flow rates of 1.0 mL min^{-1}, and the column effluent was monitored using UV as the detector. Melting points were determined with a capillary apparatus (Büchi 540) in open capillary. Flash column chromatography was performed on silica gel (Merck Kieselgel 60, 230–400 mesh ASTM). The progress of the reactions was followed by thin-layer chromatography (TLC) on 5 × 20 cm plates Merck Kieselgel 60 F254, with a layer thickness of 0.20 mm. Anhydrous sodium sulfate (Na_2SO_4) was used as drying agent for the organic phases. Organic

solvents were removed under reduced pressure at 30°C. Synthetic-purity solvents dichloromethane (DCM), acetonitrile (CH_3CN), methanol (MeOH), diethyl ether (Et_2O), diisopropyl ether (*i*-Pr_2O), dimethylformamide (DMF) and 40–60 petroleum ether (PE) were used. Dry DMF was obtained through storage on 4Å molecular sieves. Dry CH_2Cl_2 was distilled from P_2O_5 and stored on molecular sieves 4Å. Commercial starting materials were purchased from Sigma-Aldrich, Alfa Aesar, and TCI Europe. Gemcitabine hydrochloride was obtained from Hangzhou Trylead chemical technology Co. Ltd., Hangzhou, China. NO-donor acids **3a-g** were synthesised as described elsewhere. [36, 37]

General procedure for the synthesis 3',5'-O-bis-*tert*-bytoxycarbonyl-4-N-acetyl gemcitabine derivatives **4a-g**. To the solution of corresponding NO-donor acid **3a-g** (1.20 mmol) in 10 mL of toluene, 0.10 mL of $SOCl_2$ was added followed by 1 drop of dry DMF. The reaction mixture was stirred at rt until completed (TLC control). Then solvent has been discarded and the residue was dissolved in dry DCM. Acyl chloride solution was added dropwise to the solution of **2** (0.50 g, 1.06 mmol) and DIPEA (0.40 mL, 2.30 mmol) in dry DCM at 0 °C. The ice bath has been removed and the reaction mixture was stirred at rt for 24h. The solvent has been taken away and the residue was purified by flash chromatography with indicated eluent.

3',5'-O-bis-*tert*-Butoxycarbonyl-4-N-(3-nitroxy-2,2-dimethylpropionyl)gemcitabine (4a). Eluent: gradient from 85 / 15 to 70 / 30 DCM / acetone v / v. White powder. Yield: 63%. MS ESI^+: 609 $(M+H)^+$, 631 $(M+Na)^+$, 647 $(M+K)^+$. ^1H NMR ($CDCl_3$) δ (ppm): 1.36 (*s*, 6H, $2CH_3$), 1.46 (*s*, 18H, 2*t*-Bu), 4.35 – 4.44 (*m*, 3H, 4'C*H*, 5'CH_2), 5.05 – 5.12 (*m*, 1H, 3'C*H*), 6.38 – 6.43 (*m*, 1H, 1'C*H*), 7.39 (*br.s.*, 1H, C*H*Ar), 7.83 (*d*, 1H, C*H*Ar), 8.84 (*br.s.*, 1H, N*H*); ^{13}C NMR ($CDCl_3$) δ (ppm): 22.0, 22.1, 27.3, 27.5, 43.5, 63.7, 72.4 (*dd*, $^2J_{CF}$ = 33.7 Hz, $^2J_{CF}$ =17.1 Hz), 77.6 (*m*), 83.1, 84.0 (*m*), 84.6, 97.1, 120.0 (*dd*, $^1J_{CF}$ = 261.5 Hz, $^1J_{CF}$ =267.0 Hz), 144.7, 151.2, 152.7, 162.7.

3',5'-O-bis-*tert*-Butoxycarbonyl-4-N-(4-[2,3-dinitroxypropyl]-benzoyl)gemcitabine (4b). Eluent: 95 / 5 DCM / acetone v / v. White powder. Yield: 66%. MS ESI^+: 732.6 $(M+H)^+$, 754.6 $(M+Na)^+$. ^1H NMR (DMSO-d_6) δ (ppm): 1.39 (*s*, 9H, *t*-Bu), 1.42 (*s*, 9H, *t*-Bu), 3.10 (*dd*, $^3J_{HH}$ = 8.35

Hz, $^{2}J_{HH}$ = 14.77 Hz, 1H, C_6H_4CHH), 3.18 (*dd*, $^{3}J_{HH}$ = 5.46 Hz, $^{2}J_{HH}$ = 14.45 Hz, 1H, C_6H_4CHH), 4.34 – 4.44 (*m*, 3H, 4'C*H*, 5'CH_2), 4.67 (*dd*, $^{3}J_{HH}$ = 6.42 Hz, $^{2}J_{HH}$ = 12.84 Hz, 1H, O_2NOCHH), 4.93 (*dd*, $^{3}J_{HH}$ = 2.57 Hz, $^{2}J_{HH}$ = 12.84 Hz, 1H, O_2NOCHH), 5.27 (*br.s.*, 1H, 3'C*H*), 6.31 (*m*, 1H, 1'C*H*), 7.39 (*d*, 1H, CH_{Ar}), 7.43 (*d*, 2H, 2CH_{Ar}), 7.95 (*d*, 2H, 2CH_{Ar}), 8.09 (*d*, 1H, CH_{Ar}), 11.39 (*s*, 1H, N*H*); ^{13}C NMR (DMSO-d6) δ (ppm): 27.2, 27.3, 34.3, 65.0, 71.6, 73.0 (*m*), 75.9 (*m*), 80.2, 82.3, 83.9, 97.0, 121.3 (*t*, $^{1}J_{CF}$ = 281.8 Hz), 129.0, 129.4, 131.7, 140.8, 146.6, 151.2, 152.6, 154.0, 164.1, 167.2.

3',5'-O-bis-*tert*-Butoxycarbonyl-4-N-(4-[3-nitroxypropyl]-benzoyl)gemcitabine (4c). Eluent: 95 / 5 DCM / acetone v / v. White powder. Yield: 72%. MS ESI$^+$: 671.8 $(M+H)^+$, 693.8 $(M+Na)^+$, 709.7 $(M+K)^+$. ^{1}H NMR ($CDCl_3$) δ (ppm): 1.51 (*s*, 18H, 2*t*-Bu), 2.06 – 2.11 (*qi*, 2H, $OCH_2CH_2CH_2$), 2.79 – 2.83 (*m*, 2H, $OCH_2CH_2CH_2$), 4.38 – 4.49 (*m*, 5H, 4'C*H* + 5'CH_2 + CH_2ONO_2), 5.13 – 5.16 (*m*, 1H, 3'C*H*), 6.44 – 6.48 (*m*, 1H, 1'C*H*), 7.33 (*d*, 2H, 2CH_{Ar}), 7.63 (*br.s.*, 1H, CH_{Ar}), 7.91 – 7.95 (m, 3H, 3CH_{Ar}), 8.04 (d, 1H, NH); ^{13}C NMR ($CDCl_3$) δ (ppm): 27.5, 27.7, 27.9, 31.8, 63.8, 71.9, 72.6 (*m*), 77.9, 83.4, 84.9, 97.2 (*m*), 120.4 (t, $^{1}J_{CF}$ = 261.5 Hz) 128.4 (*m*), 129.0, 130.5, 130.9, 145.2 (*m*), 146.0, 146.3, 151.4, 152.9, 170.6.

3',5'-O-bis-*tert*-Butoxycarbonyl-4-N-(4-[2,3-dinitroxypropyloxy]-benzoyl)gemcitabine (4d). Eluent: 90 / 10 DCM / acetone v / v. White powder. Yield: 61%. MS ESI$^+$: 748.8 $(M+H)^+$, 770.7 $(M+Na)^+$. ^{1}H NMR ($CDCl_3$) δ (ppm): 1.52 (*s*, 18H, 2*t*-Bu), 4.31 – 4.48 (*m*, 5H, $C_6H_4CH_2$, + 4'C*H* + 5'CH_2), 4.81 (*dd*, $^{3}J_{HH}$ = 6.54 Hz, $^{2}J_{HH}$ = 13.08 Hz, 1H, O_2NOCHH), 4.95 (*dd*, $^{3}J_{HH}$ = 3.44 Hz, $^{2}J_{HH}$ = 13.08 Hz, 1H, O_2NOCHH), 5.15 (*m*, 1H, 3'C*H*), 5.64 – 5.67 ($CHONO_2$), 6.45 (*m*, 1H, 1'C*H*), 7.01 (*d*, 2H, 2CH_{Ar}), 7.65 (*br.s.*, 1H, CH_{Ar}), 7.98 (*d*, 2H, 2CH_{Ar}), 8.05 (*br.s.*, 1H, CH_{Ar}); ^{13}C NMR ($CDCl_3$) δ (ppm): 27.5, 27.7, 63.8, 64.9, 68.6, 72.3 (*m*), 76.3, 78.0, 83.5, 85.0, 114.8, 122.1 (t, $^{1}J_{CF}$ = 278.8 Hz), 129.5, 130.6, 151.4, 152.9, 160.3, 161.6.

3',5'-O-bis-*tert*-Butoxycarbonyl-4-N-(4-[3-nitroxypropyloxy]-benzoyl)gemcitabine (4e). Eluent: 95 / 5 DCM / acetone v / v. White powder. Yield: 47%. MS ESI$^+$: 687.4 $(M+H)^+$, 709.4 $(M+Na)^+$, 725.5 $(M+K)^+$. ^{1}H NMR ($CDCl_3$) δ (ppm): 1.52 (*s*, 18H, 2*t*-Bu), 2.26 (*qi*, 2H, $^{3}J_{HH}$ = 6.10

Hz, $OCH_2CH_2CH_2$), 4.15 (*t*, $^3J_{HH}$ = 6.10 Hz, 2H, $OCH_2CH_2CH_2$), 4.38 – 4.49 (*m*, 3H, 4'C*H*, 5'CH_2), 4.69 (*t*, $^3J_{HH}$ = 6.10 Hz, 2H, CH_2ONO_2), 5.13 – 5.16 (*m*, 1H, 3'C*H*), 6.46 – 6.49 (*m*, 1H, 1'C*H*), 6.98 (*d*, 2H, 2CH_{Ar}), 7.60 (*br.s.*, 1H, CH_{Ar}), 7.89 (*br.s.*, 2H, 2CH_{Ar}), 8.84 (*br.s.*, 1H, CH_{Ar}); ^{13}C NMR ($CDCl_3$) δ (ppm): 26.8, 27.5, 27.7, 63.9, 72.6 (*m*), 77.7 (*m*), 83.3, 83.9 (*m*), 84.8, 97.0 (*m*), 114.7, 120.4 (*t*, $^1J_{CF}$ = 263.0 Hz), 129.8 (*m*), 144.9, 151.4, 152.9, 162.5.

3',5'-O-bis-*tert*-Butoxycarbonyl-4-N-(5,6-dinitroxyesanoyl)gemcitabine (4f). Eluent: gradient from 95 / 5 to 90 / 10 DCM / acetone v / v. White powder. Yield: 53%. MS ESI$^+$: 684.4 $(M+H)^+$, 706.3 $(M+Na)^+$. ^{1}H NMR ($CDCl_3$) δ (ppm): 1.49 (*s*, 18H, 2*t*-Bu), 1.78 – 1.84 (*m*, 4H, 2CH_2), 2.64 – 2.70 (*m*, 2H, CH_2), 4.36 – 4.49 (*m*, 4H, CH_2ONO_2 + 5'CH_2), 4.74 – 4.78 (*m*, 1H, 4'C*H*), 5.13 – 5.16 (*m*, 1H, 3'C*H*), 5.27 – 5.34 (*m*, 1H, C*H*ONO_2), 6.37 (*br.s.*, 1H, 1'C*H*), 7.51 (*d*, 1H, CH_{Ar}), 7.86 (*d*, 1H, CH_{Ar}), 10.70 (d, 1H, N*H*); ^{13}C NMR ($CDCl_3$) δ (ppm): 19.8, 27.5, 27.7, 28.4, 36.0, 63.8, 71.1, 72.3 (*m*), 77.8 (*m*), 78.8 (*m*), 83.4, 84.9, 120.5 (*t*, $^1J_{CF}$ = 261.2 Hz), 129.8 (*m*), 144.9, 151.4, 152.9, 154.6, 172.8, 173.3.

3',5'-O-bis-*tert*-Butoxycarbonyl-4-N-(6-nitroxyesanoyl)gemcitabine (4g). Eluent: gradient from 95 / 5 to 90 / 10 DCM / acetone v / v. White powder. Yield: 55%. MS ESI$^+$: 623.6 $(M+H)^+$, 645.6 $(M+Na)^+$. ^{1}H NMR ($CDCl_3$) δ (ppm): 1.44 – 1.51 (*m*, 20H, 2*t*-Bu + CH_2), 1.69 – 1.78 (*m*, 4H, 2CH_2), 2.57 – 2.61 (*m*, 2H, CH_2), 4.37 – 4.48 (*m*, 5H, CH_2ONO_2 + 5'CH_2 + 4'C*H*), 5.12 – 5.13 (*m*, 1H, 3'C*H*), 6.43 (*br.s.*, 1H, 1'C*H*), 7.52 (*d*, 1H, CH_{Ar}), 7.86 (*d*, 1H, CH_{Ar}), 10.20 (*br.s.*, 1H, N*H*); ^{13}C NMR ($CDCl_3$) δ (ppm): 23.9, 25.0, 26.4, 27.5, 27.7, 36.8, 63.8, 72.3 (*m*), 73.0, 77.7, 83.3, 84.8, 97.5, 120.5 (*t*, $^1J_{CF}$ = 261.5 Hz), 144.7, 151.4, 152.9, 154.6, 163.6, 173.8.

General procedure for the synthesis 4-N-acetyl gemcitabine derivatives **5a-g**. To the solution of corresponding protected derivatives (4a-g) in 9.5 mL of DCM TFA (0.5 mL) was added in one portion. Reaction mixture was stirred at rt for 24h, then solvent was removed and residue was dissolved in AcOEt (20 mL). Organic solvent was washed with H_2O (20 mL), $NaHCO_3$ saturate solution (25 mL), brine. Organic phase was anidrificated and solvent was removed. The residue was

purified by flash chromatography. Obtained oil was dissolved in minimum quantity of EtOAc and product was precipitated adding Et_2O, filtered and essicated.

4-N-(3-Nitroxy-2,2-dimethylpropyonyl)gemcitabine (5a). Eluent: 95 / 5 DCM / MeOH v / v. White powder. Yield: 79%. M.p.: 164.5 – 165.5 °C. MS ESI$^+$: 409.2 $(M+H)^+$, 431.1 $(M+Na)^+$, 447 $(M+K)^+$. ^{1}H NMR (CD_3OD) δ (ppm): 1.38 (*s*, 6H, 2C*H*$_3$), 3.80 – 3.99 (*m*, 3H, 4'C*H*, 5'C*H*$_2$), 4.30 – 4.33 (*m*, 1H, 3'C*H*), 4.65 (*s*, 2H, C*H*$_2$ONO$_2$), 6.25 – 6.28 (*m*, 1H, 1'C*H*), 7.48 (*d*, 1H, C*H*$_{Ar}$), 8.38 (*d*, 1H, C*H*$_{Ar}$); ^{13}C NMR (CD_3OD) δ (ppm): 22.1, 22.1, 45.0, 60.3, 70.1 (*m*), 78.6, 83.0, 86.7 (*m*), 98.7, 124.0 (*t*, $^1J_{CF}$ = 258.7 Hz), 146.4, 157.6, 165.1, 176.9. PHPLC: > 99%(226 nm).

4-N-(4-[2,3-Dinitroxypropyl]-benzoyl)gemcitabine (5b). Eluent: 96 / 4 DCM / MeOH v / v. White powder. Yield: 59%. M.p.: 168.5-169.0 °C. MS ESI$^+$: 532.4 $(M+H)^+$, 554.4 $(M+Na)^+$. ^{1}H NMR (CD_3OD) δ (ppm): 3.19 (*m*, 2H, $C_6H_4CH_2$), 3.83 (*dd*, $^3J_{HH}$ = 2.75 Hz, $^2J_{HH}$ = 12.74 Hz, 1H, 5'C*H*H), 3.98 – 4.00 (*m*, 2H, 4'C*H*, 5'CH*H*), 4.30 – 4.34 (*m*, 1H, C*H*ONO$_2$), 4.61 (*dd*, $^3J_{HH}$ = 6.54 Hz, $^2J_{HH}$ = 13.08 Hz, 1H, O$_2$NOC*H*H), 4.93 (*dd*, $^3J_{HH}$ = 2.75 Hz, $^2J_{HH}$ = 12.74 Hz, 1H, O$_2$NOCH*H*), 5.66 – 5.70 (*m*, 1H, 3'C*H*), 6.29 (*m*, 1H, 1'C*H*), 7.50 (*d*, 2H, 2C*H*$_{Ar}$), 7.61 (*d*, 1H, 1C*H*$_{Ar}$), 7.95 (*d*, 2H, 2C*H*$_{Ar}$), 8.41 (*d*, 1H, C*H*$_{Ar}$); ^{13}C NMR (CD_3OD) δ (ppm): 36.1, 60.4, 70.5 (*m*), 72.3, 81.0, 85.9 (*m*), 96.3, 124.0 (t, $^1J_{CF}$ = 258.7 Hz), 130.6, 130.9, 131.1, 142.4, 142.6, 157.9, 167.7, 168.2. PHPLC: > 99% (226 nm).

4-N-(4-[3-Nitroxypropyl]-benzoyl)gemcitabine (5c). Eluent: 96 / 4 DCM / MeOH v / v. Yield: 80%. M.p.: 193.0-194.2 °C. MS ESI$^+$: 471.4 $(M+H)^+$, 493.4 $(M+Na)^+$. ^{1}H NMR (CD_3OD) δ (ppm): 2.04 – 2.10 (*m*, 2H, OCH$_2$C*H*$_2$CH$_2$), 2.78 – 2.84 (*m*, 2H, OC*H*$_2$), 3.77 – 4.00 (*m*, 3H, 4'C*H* + 5'C*H*2), 4.31 – 4.36 (*m*, 1H, 3'C*H*), 4.50 (t, 2H, C*H*$_2$ONO$_2$), 6.29 (*m*, 1H, 1'C*H*), 7.41 (d, 2H, 2C*H*$_{Ar}$), 7.62 (*m*, 1H, C*H*$_{Ar}$), 7.92 (*d*, 2H, 2C*H*$_{Ar}$), 8.41 (*m*, 1H, C*H*$_{Ar}$); ^{13}C NMR (CD_3OD) δ (ppm): 29.3, 32.8, 60.4, 70.3 (*m*), 73.8, 83.1, 86.6 (*m*), 96.4, 98.8, 124.1 (*t*, $^1J_{CF}$ = 258.7 Hz), 126.8, 130.1, 131.0, 132.7, 142.6, 146.2, 148.2, 157.8, 165.5, 169.0. PHPLC: > 99%(226 nm).

4-N-(4-[2,3-Dinitroxypropyloxy]-benzoyl)gemcitabine (5d). Eluent: 96 / 4 DCM / MeOH v / v. Yield 72%. M.p.: 115.5-124.0 °C. MS ESI$^+$: 516.4 $(M+H)^+$, 538.4 $(M+Na)^+$. ^{1}H NMR (CD_3OD) δ (ppm): 3.82 – 4.00 (*m*, 3H, 4'C*H*, 5'CH_2), 4.32 – 4.48 (*m*, 3H, $C_6H_4CH_2$ + C*H*ONO_2), 4.81 – 4.91 (*m*, 1H, C*H*HONO_2), 5.04 (*dd*, $^3J_{HH}$ = 3.10 Hz, $^2J_{HH}$ = 13.08 Hz, 1H, CH*H*ONO_2), 5.80 – 5.82 (*m*, 1H, 3'C*H*), 6.28 (*m*, 1H, 1'C*H*), 7.11 (*d*, 2H, 2CH_{Ar}), 7.61 (*d*, 1H, 1CH_{Ar}), 7.99 (*d*, 2H, 2CH_{Ar}), 8.39 (*d*, 1H, CH_{Ar}); ^{13}C NMR (CD_3OD) δ (ppm): 60.4, 66.7, 70.3 (*m*), 70.9, 83.0, 86.6 (*m*), 98.8, 115.8, 125.8 (*t*, $^1J_{CF}$ = 258.7 Hz), 131.7, 132.8, 146.1, 157.8, 163.4, 165.5, 168.4. PHPLC: 99% (226 nm).

4-N-(4-[3-Nitroxypropyloxy]-benzoyl)gemcitabine (5e). Eluent: 96 / 4 DCM / MeOH v / v. Yield: 69%. M.p.: 139.0-140.0 °C. MS ESI$^+$: 487.4 $(M+H)^+$, 509.4 $(M+Na)^+$, 525.5 $(M+K)^+$. ^{1}H NMR (CD_3OD) δ (ppm): 2.23 (*m*, 2H, $OCH_2CH_2CH_2$), 3.83 (*m*, 1H, 5'C*H*H), 3.89 (*m*, 2H, 4'C*H* + 5'CH*H*), 4.17 (t, $^3J_{HH}$ = 5.78 Hz, 2H, CH_2O), 4.33 (*m*, 1H, 3'C*H*), 4.69 (*t*, $^3J_{HH}$ = 6.10 Hz, 2H, CH_2ONO_2), 6.28 (*m*, 1H, 1'C*H*), 7.05 (*d*, 2H, 2CH_{Ar}), 7.60 (*m*, 1H, CH_{Ar}), 7.94 (*d*, 2H, 2CH_{Ar}), 8.38 (*m*, 1H, CH_{Ar}); ^{13}C NMR (CD_3OD) δ (ppm): 28.1, 60.4, 65.7, 70.3 (*m*), 71.6, 83.3, 86.6 (*m*), 98.8, 115.7, 124.1 (t, $^1J_{CF}$ = 258.7 Hz), 126.8, 131.6, 146.1, 157.8, 164.3, 165.6, 168.4. PPLC: > 99% (226 nm).

4-N-(5,6-Dinitroxyhexanoyl)gemcitabine (5f). Eluent: 96 / 4 DCM / MeOH v / v. Yield: 68%. M.p.: 109.0-110.0°C. MS ESI$^+$: 484.4 $(M+H)^+$, 506.3 $(M+Na)^+$. ^{1}H NMR (CD_3OD) δ (ppm): 1.68 – 1.81 (*m*, 4H, 2CH_2), 2.37 – 2.53 (*m*, 2H, CH_2), 3.74 – 3.96 (*m*, 4H, CH_2ONO_2 + 5'CH_2), 4.20 – 4.28 (m, 1H, 4'C*H*), 4.55 – 4.59 (m, 1H, 3'C*H*), 4.87 – 4.89 (*m*, C*H*ONO_2), 5.36 – 5.39 (*m*, 1H, C*H*ONO_2), 5.87 (*d*, 1H, CH_{Ar}), 6.18 – 6.25 (m, 1H, 1'C*H*), 7.81 (d, 1H, CH_{Ar}); *13*C NMR (CD_3OD) δ (ppm): 21.5, 29.6, 34.1, 37.3, 60.7, 70.5 (*m*), 73.0, 81.0, 82.5, 86.0 (*m*), 96.5, 98.4, 121.1, 142.6, 146.1, 157.9, 164.9, 167.9, 175.3. PHPLC: > 99% (226 nm).

4-N-(6-Nitroxyhexanoyl)gemcitabine (5g). Eluent: 90 / 10 DCM / MeOH v / v. Yield: 44%. M.p.: 142.5-144.5 °C. MS ESI$^+$: 423.4 $(M+H)^+$, 445.4 $(M+Na)^+$, 461.4 $(M+K)^+$. ^{1}H NMR (CD_3OD) δ (ppm): 1.45 – 1.49 (*m*, 2H, CH_2), 1.69 – 1.78 (*m*, 4H, 2CH_2), 2.49 (*t*, $^3J_{HH}$ = 6.42 Hz, 2H, OCCH_2), 3.80 – 3.99 (*m*, 3H, 5'CH_2 + 4'C*H*), 4.27– 4.33 (*m*, 1H, 3'C*H*), 4.50 (*t*, 2H, CH_2ONO_2), 6.25 – 6.27

(*m*, 1H, 1'C*H*), 7.48 (*d*, 1H, C*H*$_{Ar}$), 8.33 (*d*, 1H, C*H*$_{Ar}$); ^{13}C NMR (CD_3OD) δ (ppm): 25.5, 26.4, 27.7, 37.9, 60.4, 70.3 (*m*), 74.5, 83.0, 86.8 (*m*), 98.4, 124.1 (*t*, $^{1}J_{CF}$ = 258.7 Hz), 146.1, 157.8, 164.9, 175.8. PHPLC: 97% (226 nm).

Lipophilicity. ClogP values were calculated using the Bio-Loom program for Windows, Version 1.5 (BioByte). The partition coefficients between n-octanol and PBS at pH 7.4 (log $D^{7.4}$), were obtained using the shake-flask technique at room temperature. In the shake flask experiments, 50 mM of phosphate buffered saline at pH 7.4 (ionic strength adjusted to 0.15 M with KCl) was used as the aqueous phase. The organic (n-octanol), and aqueous phases were mutually saturated by shaking for 4 h. The compounds were solubilised in the buffered aqueous phase at concentrations of either 0.1 mM or 0.05 mM, depending on their solubility, and appropriate amounts of n-octanol were added. The two phases were shaken for about 20 min, by which time the partitioning equilibrium of solutes had been reached, and then centrifuged (10000 rpm, 10 min). The concentration of the solutes was measured in the aqueous phase by UV spectrophotometer (UV-2501PC, Shimadzu); absorbance values (recorded for each compound at the wavelength of maximum absorption), were interpolated in calibration curves obtained using standard solutions of the compounds (r^2 >0.99). Each log D value is an average of at least six measurements.

Stability in PBS and in human serum. Stability of compounds was determined first in phosphate-buffered saline (PBS, pH 7.4): DMSO stock solutions of compounds (10 mM) were diluted at 100 μM concentration in PBS and solutions were incubated at 37 °C in an orbital shaker (350 rpm) for 24 h. A dedicated sample was prepared for each incubation time considered (0, 1, 6, 17 and 24 hours). At each time point, the samples were mixed and filtered through a PTFE 0.45μm filter (VWR); the solutions were analyzed by RP-HPLC (see below). Each experiment was independently repeated at least three times. The results are expressed as % of unmodified compound at 24 h. To evaluate the enzymatic stability a solution of the compounds in DMSO was added to human serum (sterile-filtered from human male AB plasma, Sigma-Aldrich), to obtain the 100 μM final concentration with 1% of

DMSO. The resulting solution was shaken in an orbital shaker at 37°C for 24 h. At appropriate time intervals (0, 1, 6, 17 and 24 hours), 200 µL of the reaction mixture were withdrawn and added to 200 µL of acetonitrile 0.1% HCOOH in order to deproteinize the serum. The samples were vortexed, sonicated for 3 min and then centrifuged for 5 min at 2500 x g. The clear supernatant was filtered and analyzed by RP-HPLC. The results are expressed as % of unmodified compound at 24 h.

HPLC analyses were performed with a HP 1200 chromatograph system (Agilent Technologies, Palo Alto, CA, USA) equipped with a quaternary pump (model G1311A), a membrane degasser (G1322A), a multiple wavelength UV detector (MWD, model G1365D), a thermostated column compartment (model G1316A), integrated in the HP1200 system. Data analysis was performed using a HP ChemStation system (Agilent Technologies). The samples were eluted on a Nucleosil 100-5 C18 HD column (250 × 4.6 mm, 5 µm, Macherey-Nagel). The injection volume was 20 µL (Rheodyne, Cotati, CA). The mobile phase consisting of acetonitrile 0.1% HCOOH (solvent A) and water 0.1% HCOOH (solvent B) at flow-rate = 1.0 mL/min with gradient conditions: 10% A until 4 min, from 10 to 50% A between 4 and 6 min, 50% A between 6 and 15 min, and from 50 to 10% A between 15 and 20 min. The column effluent was monitored by MWD at 250, 270 and 292 nm referenced against an 800 nm wavelength according to the maximum absorption of each compound. Quantitation of the compounds was done using calibration curves obtained using standard solutions of compounds (linearity determined in a concentration range of 1-150 µM; $r^2 > 0.99$).

Liposome preparation

All the phospholipids were provided by Avanti Polar-Lipids distributed by Sigma-Chemical Co (St. Louis, MO), cholesterol, all the other chemicals were obtained from Sigma Chemicals Co. Liposomes containing 5b (**Lipo 5b**) were prepared by thin lipid film hydration and extrusion method. Briefly, a chloroform solution of 1,2-distearoyl-*sn*-glycero-3-phosphocholine (DSPC), cholesterol (Chol), 1,2-distearoyl-*sn*-glycero-3-phosphoethanolamine-*N*-[amino(polyethylene glycol)-2000]

(mPEG-DSPE, ammonium salt) at a molar ratio of 65:30:5 and containing **5b** (28% ratio mol drug/mol lipid) was evaporated and the resulting lipid film was dried under vacuum overnight. The thin film was then hydrated with a 20 mM 4-(2-hydroxyethyl)piperazine-1-ethanesulforic acid (HEPES) buffer (pH 7.4) and the suspension was vortex mixed for 10 min and bath sonicated. The formulations were then sequentially extruded (Extruder, Lipex, Vancouver, Canada) through 400 and then 200 nm polycarbonate membrane (Costar, Corning Incorporated, NY) at a set temperature of 5°C above the phase transition temperature of the lipid mixture. Liposomal preparations were purified from non-encapsulated **5b** through chromatography on Sepharose CL-4B columns, eluting with HEPES buffer at room temperature. Liposomes were stored at 4°C.

Liposome characterization

The mean particle size and polydispersity index of the liposomes were determined at 20°C by Quasi-elastic light scattering (QELS) using a nanosizer Coulter® N4MD (Coulter Electronics, Inc., Hialeah, FL). The selected angle was 173° and the measurement was taken after dilution of the liposome suspensions in MilliQ® water. Each measurement was carried out in triplicate. The particle surface charge of liposomes was investigated by zeta potential measurements at 25 °C applying the Smoluchowski equation and using the Nanosizer Nano Z. Measurements were carried out in triplicate. Phospholipid phosphorous was assessed in each liposome preparation by phosphate assay after destruction with perchloric acid. [38] The amount of **5b** incorporated in liposomes was determined by reverse phase (RP)-HPLC with the chromatographic method described above. The liposomal formulation was diluted with CH_3CN, sonicated, vortexed, and filtered through 0.45 μm PTFE filters (Alltech). Quantitation of compound **5b** was done using calibration curve obtained using standard solutions of compound chromatographed in the same experimental conditions (linearity determined in a concentration range of 1-150 μM; $r^2 > 0.99$).

Liposomal preparations were analyzed for physical stability in the storage conditions evaluating at different time intervals: diameter, zeta potential and drug leakage at 4°C. Drug leakage was determined submitting 200 µl of liposomes to purification through chromatography on Sepharose CL-4B columns, eluting with HEPES buffer, and re-analyzing for drug and phospholipid content as described above. A change in content was interpreted as an indication of liposome instability.

To evaluate **5b** release in fetal calf serum (FCS) the formulations were diluted 1:2.5 with FCS and incubated at 37°C for various periods of time. The **5b**-loaded liposomes were separated from the leaked drug as previously described. Then, the drug and lipid content was measured in the collected liposomal fractions and compared with initial values. For comparison, a drug leakage study was also performed in HEPES buffer at 37°C.

For DSC analysis about 15 mg of hydrated samples suspension were introduced into a 40 µl aluminium pan and analyzed. DSC runs were conducted from 25 °C to 80 °C at a rate of 5 °C/min under constant nitrogen stream (50 ml/min). The main transition temperature (Tm) was determined as the onset temperature of the highest peak.

Cell culture

Pancreatic adenocarcinoma PANC-1 and MIAPaCa-2 cell lines were grown in DMEM medium (Gibco, Thermo Fisher), supplemented with 10% FBS and 50 µg/ml gentamicin sulfate (BioWhittaker, Lonza), and incubated at 37 °C with 5% CO_2.

Cell proliferation assay

Cells were seeded in 96-well plates (5 x 10^3 cells/well), 24h later treated with various compounds and further incubated for the indicated times (see legends to figures). At the end of the treatments cells were stained and fixed with a crystal violet solution containing formaldehyde (for a solution of 100mL: 750 mg of violet crystal powder, 250 mg of NaCl, 4.7 mL of 37% formaldehyde,

50 mL of ethanol and 45.3 mL of bidistilled water) (Sigma, Milan, Italy). The dye was solubilized in PBS containing 1% SDS and measured photometrically at 595 nm absorbance by a microplate reader (GENios Pro, Tecan, Milan, Italy) to determine cell growth.

DNA damage assay

The genotoxic damages were evaluated by the Single Cell Gel Electrophoresis assay (Comet assay), as reported previously[39]. Images were quantified by the CometScore software (TriTek Corp., Sumerduck, VA). The DNA dependent pro-apoptotic damage was measured using the TUNEL Assay Kit - BrdU-Red (Abcam, Cambridge, MA), as per manufacturer's instruction. The image quantification was performed using the ImageJ software (https://imagej.nih.gov/ij/), counting 10 microscopic fields, with a minimum of 20 cells/field.

Intracellular analysis of GFP

Cells were seeded in 96-well plates (5 x 10^3 cells/well) and, the day after, treated with 10 µL or 100 µL of GFP encapsulated in liposome for 48h. Cells were washed with PBS to remove liposomes which not entered in cells. GFP fluorescence (em. 485 nm and ex. 535 nm) was measured in HANKS solution by multimode plate reader (GENios Pro, Tecan, Milan, Italy). Values were normalized on cell proliferation by the crystal violet assay.

Intracellular drug accumulation assay

PANC-1 cellular samples derived from compound incubation were diluted 3:1 with acetonitrile 0.1% HCOOH; the mixture was sonicated, centrifuged for 10 min at 2150 g, filtered (0.45 µm PTFE) and analyzed by RP-HPLC. The concentration of compound was normalized to the protein content and expressed as nmol compound/mg cell proteins.

HPLC analyses were performed with a HP 1200 chromatograph system (Agilent Technologies, Palo Alto, CA, USA) previously described. The samples were eluted on an Aquasil C18 column (200 × 4.6 mm, 5 μm, Thermo). The column effluent was monitored by MWD at 270 nm referenced against an 800 nm wavelength. Quantitation of compound **5b** was done using calibration curve obtained using standard solutions of compound (linearity determined in a concentration range of 0.1-100 μM; $r^2 > 0.99$).

Cell cycle analysis

Cells were washed twice with fresh phosphate buffered saline (PBS), incubated in 0.5 mL ice-cold 70% v/v ethanol for 15 min, then centrifuged at 1200 x g for 5 min at 4°C and rinsed with 0.3 mL citrate buffer (50 mM Na2HPO4, 25 mM sodium citrate, and 0.01% v/v Triton X-100) containing 10 mg/mL propidium iodide and 1 mg/mL RNAse (from bovine pancreas). After 15-min incubation in the dark, the intracellular fluorescence was detected by an EasyCyte flow cytometer (Becton Dickinson, Bedford, MA). For each analysis, 1 x 10^4 events were collected and analyzed by the Incyte software (Becton Dickinson).

Apoptosis assay

Cells were seeded in 96-well plates (5 x 10^3 cells/well) and, the day after, treated with drugs at the indicated concentrations for 48h. At the end of the treatments, cells were fixed with 4% paraformaldehyde in PBS at room temperature for 30 min, then washed twice with PBS and stained with annexinV/FITC (Bender Med- System, Milan, Italy) in binding buffer (10 mM HEPES/NaOH pH 7.4, 140 mM NaCl, and 2.5 mM $CaCl_2$) for 10 min at room temperature in the dark. Finally, cells were washed with binding buffer solution and fluorescence was measured by using a multimode plate reader with excitation and emission filters at 485 nm and 535 nm respectively (GENios Pro, Tecan, Milan, Italy). The values were normalized on cell proliferation by crystal violet assay.

Western blotting

Cells were treated, harvested and washed in PBS, and re-suspended in RIPA buffer (50 mM Tris–HCl pH 7.5, 150 mM NaCl, 1 % Igepal CA-630, 0.5 % Na-Doc, 0.1 % SDS, 1 mM Na_3VO_4, 1 mM NaF, 2.5 mM EDTA, 1 mM PMSF, and 1x protease inhibitor cocktail). After incubation on ice for 30 min, the lysate was centrifuged at 14,000 g for 10 min at 4°C and the supernatant collected for the analysis. Protein concentration was quantified by Bradford reagent (Pierce, Milan, Italy) using bovine serum albumin as a standard. Protein extracts (30 μg/lane) were loaded in a 12% SDS–polyacrylamide gel to be resolved and so electro-blotted onto PVDF membranes (Millipore, Milan, Italy). Membranes were incubated with blocking solution (5% low-fat milk in TBST (100 mM Tris pH 7.5, 0.9 % NaCl, 0.1 % Tween 20) for 1 h at room temperature and probed overnight at 4°C with a primary Bim (C34C5) Rabbit mAb (Cell Signaling Technology) or GAPDH (14C10) Rabbit mAb (Cell Signaling Technology). Immunodetection was carried out using chemiluminescent substrates (Amersham Pharmacia Biotech, Milan, Italy) and recorded using a Hyperfilm ECL (Amersham Pharmacia Biotech).

Analysis of intracellular NO

Diaminofluorescein-FM diacetate (DAF-FM) probe (Sigma) was used to quantify intracellular NO. Cells were plated in 96-well plates (5×10^3 cells/well). 24 h later, the medium was changed with DMEM w/o serum and phenol red and cells were incubated with Nω-Nitro-L-arginine methyl ester hydrochloride (L-NAME) (Sigma) for 15 min at 37°C (as describe in figure legend), then, 10 μM DAF-FM for 30 min at 37 °C. Cells were washed with PBS to remove the probe which not entered in cells. Finally, cells were treated with pro-drugs and PTIO (Sigma). After 12 h, DAF-FM fluorescence was measured (λ_{exc} 485 nm and λ_{em} 535 nm) by a multimode plate reader (GENios Pro, Tecan, Milan, Italy). Values were normalized on cell proliferation by the crystal violet assay.

MRP5 detection, nitration/nitrosylation and activity

For the detection of MRP5 total amount, cells were rinsed with lysis buffer (50 mM Tris-HCl, 1mM EDTA, 1mM EGTA, 150mM NaCl, 1% v/v Triton-X100; pH 7.4), supplemented with the protease inhibitor cocktail III (Cabiochem, La Jolla, CA), sonicated and clarified at 13000×g, for 10 min at 4 °C. Protein extracts (20 μg) were subjected to SDS-PAGE and probed with an anti-MRP5/ABCC5 antibody (Abcam, Cambridge) or with an anti-actin antibody (Sigma Chemicals. Co.).

For the measurement of nitration and activity of MRP5, membrane-enriched fraction was prepared by ultracentrifugation as described.[40] To detect nitrated or nitrosylated MRP5, 100 μg of proteins from membrane fraction were immuno-precipitated overnight with anti-nitrotyrosine antibody (Millipore, Burlington, MA) or an anti-nitroso-cysteine antibody (Abcam), using 25 μL Pure Proteome Beads A/G (Millipore), then subjected to immunoblotting and probed with the anti-MRP5 antibody. The membranes were probed with the horseradish peroxidase-conjugated secondary antibodies (Bio-Rad), washed with Tris-buffered saline (TBS)/Tween 0.01% v/v. Proteins were detected by enhanced chemiluminescence (Bio-Rad Laboratories). Blot images were acquired with a ChemiDocTM Touch Imaging System device (Bio-Rad Laboratories).

MRP5 activity was measured by incubating 100 μg of immune-precipitated MRP5 for 30 min at 37°C with 50 μL of the reaction mix (25 mM Tris/HCl, 3 mM ATP, 50 mM KCl, 2.5 mM MgSO4, 3 mM dithiothreitol, 0.5 mM EGTA, 2 mM ouabain, 3 mM NaN3; pH 7.0). The reaction was stopped by adding 0.2 mL ice-cold stopping buffer (0.2% w/v ammonium molybdate, 1.3% v/v H2SO4, 0.9% w/v SDS, 2.3% w/v trichloroacetic acid, 1% w/v ascorbic acid). After a 30-min incubation at room temperature, the absorbance of the phosphate hydrolyzed from ATP was measured at 620 nm, using a Synergy HT Multi-Mode Microplate Reader (Bio-Tek Instruments, Winooski, VT). The absorbance was converted into μmol hydrolyzed phosphate/min/mg proteins, according to the titration curve previously prepared with serial dilutions (100 μM-0.1 nM) of $NaHPO_4$.

MRP5 silencing

1 x 10^5 cells were treated with 10 nM of three unique 27mer-siRNA duplexes, targeting MRP5 (#SR306772; Origene, Rockville, MD) or with a Trilencer-27 Universal scrambled negative control siRNA duplex (#SR30004; Origene), as per manufacturer's instructions. The efficiency of silencing was verified by immunoblotting.

Statistical analysis

The experimental data were subjected to computerized statistical analysis using the commands standard deviation and standard error of the mean in Excel. T-student test was used to calculate the experimental significance. The data were considered statistically significant if it has values of $p < 0.05$.

RESULTS

Different GEM cytotoxic effect on GEM-resistant and GEM-sensitive cell lines

As demonstrated in previous studies, the response of different PDAC cell lines to GEM treatment is basically heterogeneous and different mechanisms of chemoresistance are associated to the reduced antitumoral effect of GEM [14,15]. In **figure 1**, we show that GEM treatment determined a different intensity of response in PANC-1 and MIAPaCa-2 PDAC cell lines. Indeed, 48 hours of GEM treatment determined ~20% cell growth inhibition and ~15% of damaged DNA in PANC-1 cells (figure 1A), while it determined ~50% cell growth inhibition and ~35% of damaged DNA in MIAPaCa-2 cells (figure 1B). Representative imagines of the comet assay performed in the two PDAC cell lines treated with GEM are reported in figure 1C. These data support the usage of PANC-1 cells as a model of GEM-R PDAC cells, as compared to GEM-S MIAPaCa2 PDAC cells.

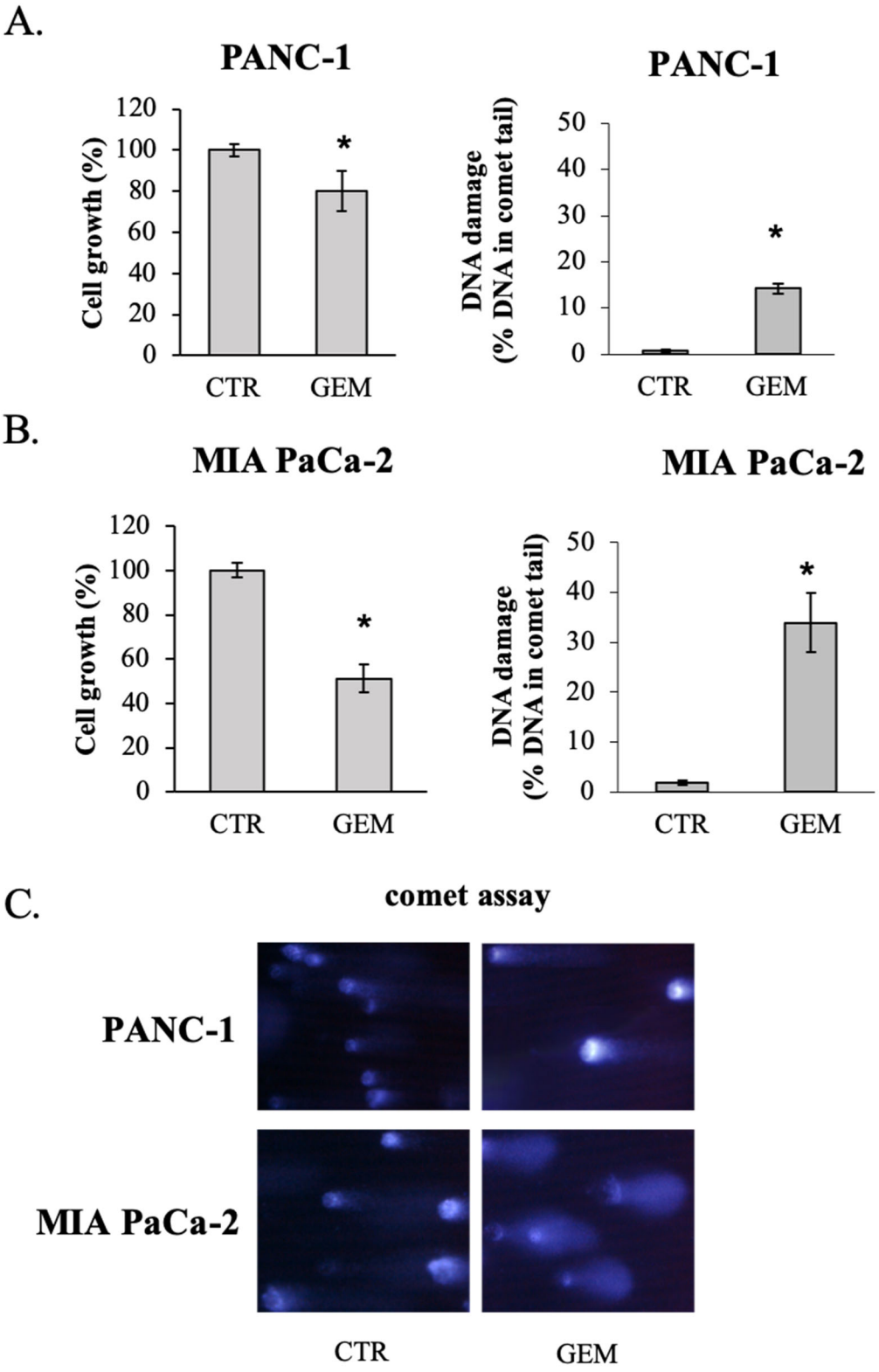

Figure 1. Cytotoxicity of GEM in PANC-1 and MIA PaCa-2 PDAC cell lines. PANC-1 (A) and MIA PaCa-2 (B) cells were treated with 100 μM GEM for 48h. C) Representative imagines of the comet assay in PANC-1 and MIA PaCa-2 cells treated with with 100

μM GEM for 48h. Measurements were performed in triplicate and data are presented as means ± SD (n = 3). Student's t-test: *p < 0.05 GEM versus CTR.

The combined treatment of GEM and NO-donor increases the cytotoxic effect in GEM-R cells

To investigate whether the addition of NO-donors to GEM treatment increased the cytotoxic effects on PDAC cells we performed cell growth assay on both PANC-1 and MIAPaCa-2 cell lines using increasing concentrations of GEM in association to a non-toxic concentration of the NO-donor diethylamine NONOate. **Figure 2** shows that the combined treatment GEM + NO-donor decreased PANC-1 cell growth as compared to GEM treatment alone (panel A), while the same combined treatment didn't enhance cytotoxicity of GEM in MIAPaCa-2 cells (panel B). These data suggest that the intracellular release of NO may favor the effect of GEM in chemoresistant PDAC cells, thus providing a rationale for further investigations with novel synthetic NO-GEM pro-drugs.

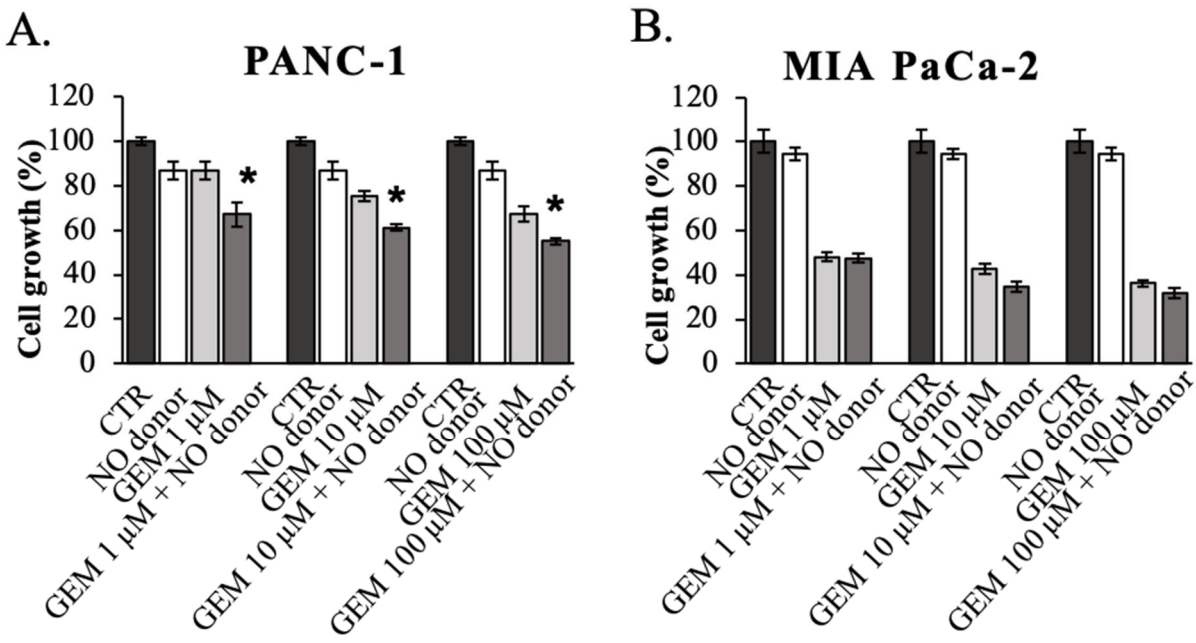

Figure 2. GEM + NO donor combined treatment inhibits GEM-R PANC-1 cell growth as compared to single treatments. PANC-1 (A) and MIA PACa-2 (B) cells were treated with increasing concentrations of GEM and/or 100 μM of NO-donor. Measurements were performed in triplicate and data are presented as means ± SD (n = 3). Student's t-test: *p < 0.05 GEM + NO donor versus GEM.

Synthesis of novel NO-GEM pro-drugs

We synthetized seven different NO-GEM pro-drugs to be tested in GEM-R and GEM-S PDAC cells. The scheme of NO-GEM pro-drugs synthesis is reported in **figure 3**. Briefly, GEM hydrochloride (**1**) was protected with tert-butoxycarbonyl group synthesis by the reaction with an excess of di-tert-butyldicarbonate in the presence of KOH in dioxane solution (**2**) following previously reported procedure.[16] NO-donor acids (**3a-g**) were activated by the treatment with $SOCl_2$ in toluene in the presence of 1 drop of DMF. Obtained acyl chlorides were coupled with 3',5'-O-bis-tert-bytoxycarbonyl derivative 2 in CH_2Cl_2 solution. Finally, the deprotection of compounds **4a-g** by 5% TFA in CH_2Cl_2 resulted in the production of desired NO-donor GEM prodrugs **5a-g**. All NO-donor GEM prodrugs and GEM as reference were characterized for their lipophilicity: the NO-donor GEM pro-drugs showed an optimal lipophilic-hydrophilic balance, which should ensure good cells permeation. All compounds were also characterized for their chemical and enzymatic stability: all compounds, except for 5a, showed a good stability both in phosphate buffered saline (PBS) and in human serum; in these conditions GEM and NO-donor substructure were the main degradation products and NO release was not observed. The results are shown in **supplementary figure 1.**

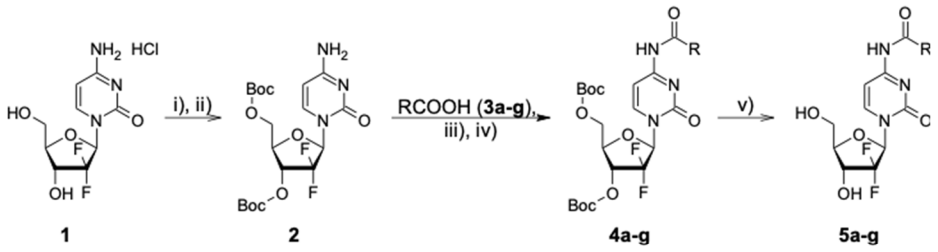

a) R = $C(CH_3)_2CH_2ONO_2$;
b) R = *p*-$C_6H_4CH_2CH(ONO_2)CH_2ONO_2$;
c) R = *p*-$C_6H_4CH_2CH_2CH_2ONO_2$;
d) R = *p*-$C_6H_4OCH_2CH(ONO_2)CH_2ONO_2$;
e) R = *p*-$C_6H_4OCH_2CH_2CH_2ONO_2$;
f) R = $(CH_2)_3CH(ONO_2)CH_2ONO_2$;
g) R = $(CH_2)_4CH_2ONO_2$.

Figure 3. Synthesis process steps of the seven NO-GEM pro-drugs starting from GEM.

Selection of the most effective NO-GEM prodrug synthesized

We performed cell growth assay to investigate the effect of the synthetized NO-GEM pro-drugs and to compare them to the GEM-based standard treatment in both PDAC cell lines. Although tested pro-drugs determined a quite similar effect on cell growth after 48 hours of cellular treatment, we selected **5b** as the most active NO-GEM pro-drug in GEM-R PANC1 cells (**figure 4A**), while no improvement was observed in GEM-S MIAPaCa-2 cells as compared to GEM (**figure 4B**). To further investigate the enhanced antiproliferative effect of **5b** in chemoresistant cells we performed a long-term cell proliferation assay. Cells were treated with a single pulse treatment for 24 hours with GEM or **5b** and, after drug removal, cell growth was analyzed at different time points until 120 hours (5 days) from the beginning of the treatment. The results shown in **figures 4C** and **4D** confirm that **5b** was significantly more cytotoxic than GEM in chemoresistant PANC-1 cells, while its effect in GEM-S MIAPaCa-2 cells was basically similar to that determined by GEM treatment.

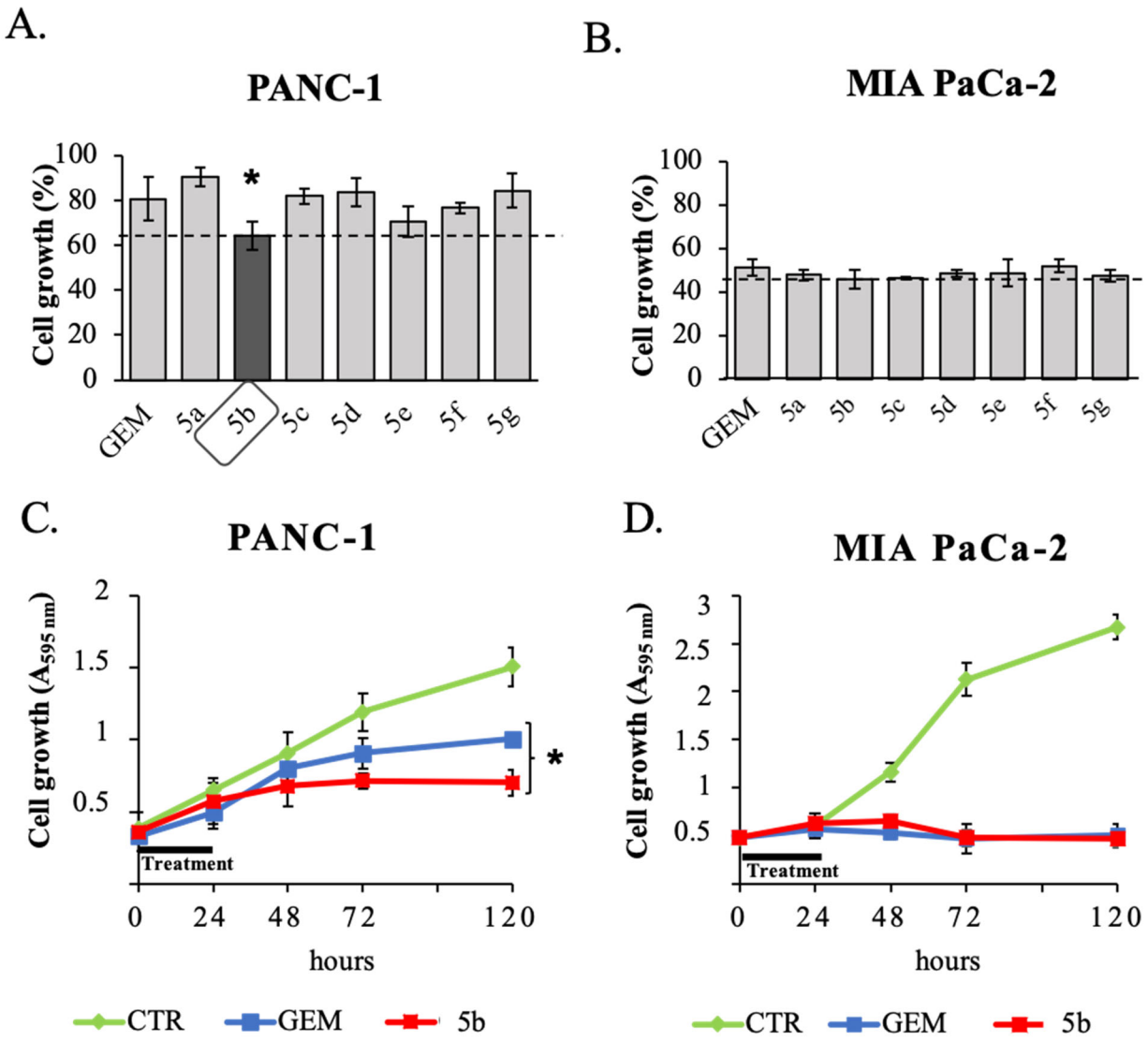

Figure 4. The compound 5b inhibits PANC-1 cell growth more than GEM. Comparison of the cytotoxic effect of GEM and of the seven new-synthesized NO-GEM pro-drugs in PANC-1 (A) and MIA PACa-2 (B) cells treated with 100 µM of pro-drugs for 48h. Long-term cytotoxicity of 10 µM GEM or 5b after a 24h pulse treatment in PANC-1 (C) and MIA PACa-2 (D) cells. Measurements were performed in triplicate and data are presented as means ± SD (n = 3). Student's t-test: *p < 0.05 5b versus GEM.

Preparation and characterization of liposomes and intracellular delivery of 5b compound

In order to facilitate the intracellular uptake of the novel pro-drug and minimize the side effects, **5b** was encapsulated in liposomes. Liposomes containing **5b** (**Lipo 5b**) were prepared by hydration of the drug-lipid film followed by extrusion through polycarbonate filters to obtain

homogenous small unilamellar vesicles. The physicochemical characteristics of the different formulations are summarized in **Table 1**. Liposomes showed dimension around 170 nm, a low polydispersity index (0.05, indicating a narrow and homogenous size distribution) and negative zeta potential value. After 4 weeks of storage in HEPES buffer at 4 °C all the formulations still conserved 80% of the initial **5b** content; over this period no appreciable size and/or zeta potential change, no precipitation or liposomes aggregation were observed. The leakage of **5b** from liposomes was evaluated in FCS and HEPES buffer at 37°C: 50% of the compound was released after 72 hours in buffer and after 48 hours in serum and nor GEM neither other degradation products from encapsulated **5b** were detected. Furthermore, the thermal changes caused by the incorporation of **5b** in the phospholipid bilayer were investigated by DSC (**figure 5A**). The thermogram of pure DSPC showed the main transition peak at T_{onset} 54.1 °C and no significant changes in the transition temperature were observed in the presence of mPEG-DSPE (T_{onset} 53.8 °C). On the other hand, with **5b** the main transition was shifted to lower temperatures, T_{onset} 50.6 °C, and the melting temperature peak was broader indicating that **5b** interacts with the liposome bilayer through hydrophobic interactions and thus perturbing the phase transition behavior. Incorporation of cholesterol in DSPC liposomes dramatically perturbed the phase transition: the main transition was abolished indicating a strong interaction of cholesterol with liposomes' bilayer that altered the calorimetric profile.

In addition, we tested the transport ability of liposomes containing the green fluorescent protein (GFP) and we measured its emission intensity inside the cells after 48 hours. The increasing concentration of GFP into the cells suggests that liposomes are a valuable method for drug delivery in our experimental system (**figure 5B**). Then, a drug-stability assay was performed in order to measure the concentration of GEM effectively released into PANC-1 cells treated with different concentrations of **5b** or **Lipo 5b** for a short period (4 hours) or a long period (24 hours). **Figure 5C** shows that liposome encapsulation of **5b** resulted in higher accumulation of GEM into the cells than non-encapsulated drug treatment at each experimental condition tested.

A.

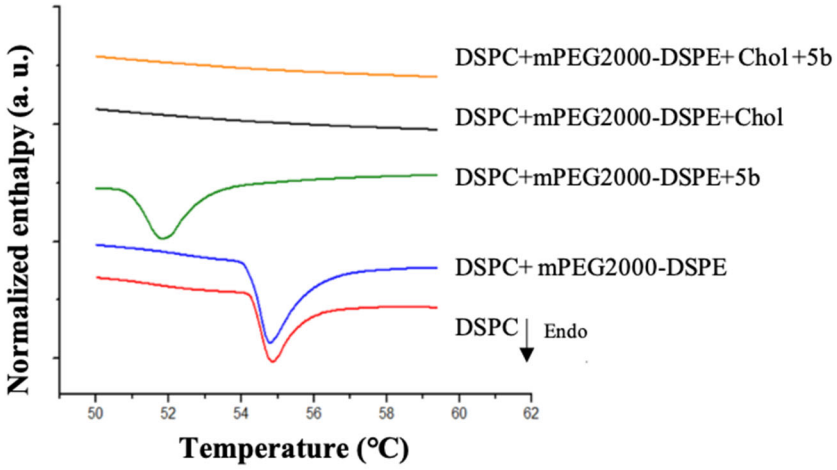

	Onset (°C)
DSPC	54.1
DSPC+ mPEG-DSPE	53.8
DSPC + mPEG-DSPE + 5b	51.8
DSPC + mPEG-DSPE + Chol	/
DSPC + mPEG-DSPE + Chol + 5b	/

B.

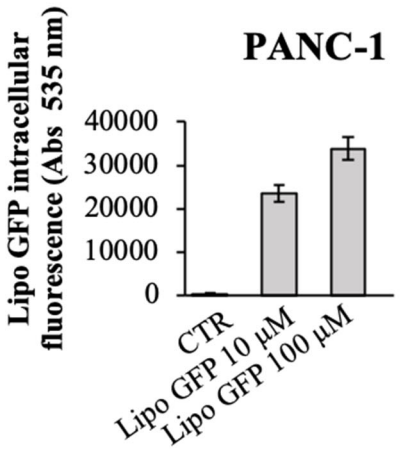

C.

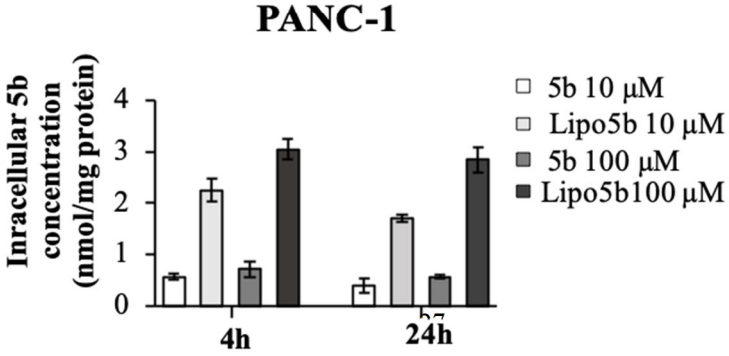

Figure 5. Analysis of liposomes' stability and intracellular drug delivery. A) Analysis of liposomes' stability. B) Intracellular amount of GFP-released by liposomes after PANC-1 cell treatment with Lipo GFP for 48h. C) Intracellular amount of 5b compound after cell treatment with 10 or 100 μM of 5b or Lipo 5b for 4h or 24h in PANC-1 cells. Measurements were performed in triplicate and data are presented as means ± SD (n = 3). Student's t-test: *p < 0.05 Lipo 5b versus 5b.

Table 1. Characteristics of liposomes containing Lipo 5b (means ± SD; n=3).

Formulation	Mean particle size (nm ± SD)	Polydispersity Index	Zeta potential (mV ± SD)	Entrapment efficiency (%) *
Lipo 5b	172 ± 3.1	0.051	−8. 7 ± 0.6	39.3 ± 2.6

*ratio between drug/lipid molar ratio after purification and drug/lipid molar ratio after extrusion.

The delivery of 5b encapsulated in liposomes increases its cytotoxic effects in GEM-R cells

The effect of encapsulated **5b** (**Lipo 5b**) was evaluated in comparison to the standard GEM and the **5b** pro-drug to prove that its higher intracellular delivery may result in higher cytotoxic effects. As control, we tested the effects of empty liposomes on cell growth without observing any significant alterations (data not shown). **Figure 6** shows that **Lipo 5b** determined a higher inhibition of cell growth (panel A) and stimulation of apoptosis (panel B) in PANC-1 cells, as compared to GEM or **5b** treatments. On the other side, **Lipo 5b** failed to improve the cytotoxic effects of **5b** in MIAPaCa-2 cells, suggesting that liposome delivery is a useful approach for a further enhancement of **5b** effect in GEM-R PDAC cells. Accordingly, TUNEL assay confirmed that **5b** encapsulation in liposomes strongly enhanced apoptosis in PANC-1 cells, without any improvements in MIAPaCa-2 cells (**figure 6C**). Moreover, we demonstrated that the apoptotic response of PANC-1 cells to GEM, **5b** or **Lipo 5b** is strictly associated to the concomitant stimulation of Bim expression at both mRNA and protein levels (**figure 6D**), suggesting the triggering of the intrinsic apoptotic pathway after GEM-R cell treatment with **Lipo 5b**. Concerning a possible involvement of the cytostatic effect on cell growth inhibition induced by drugs, we analyzed the percentage of cells in the various phases of the cell cycle after treatments. **Supplementary figure 2** shows that GEM, **5b** and **Lipo 5b** didn't

significantly alter cell cycle distribution in PANC-1 cells, while treatments increased the percentage of the GEM-S MIAPaCa-2 cells in the pre-G0 hypo-diploid phase, a phenomenon associated with the induction of apoptosis in these cells.

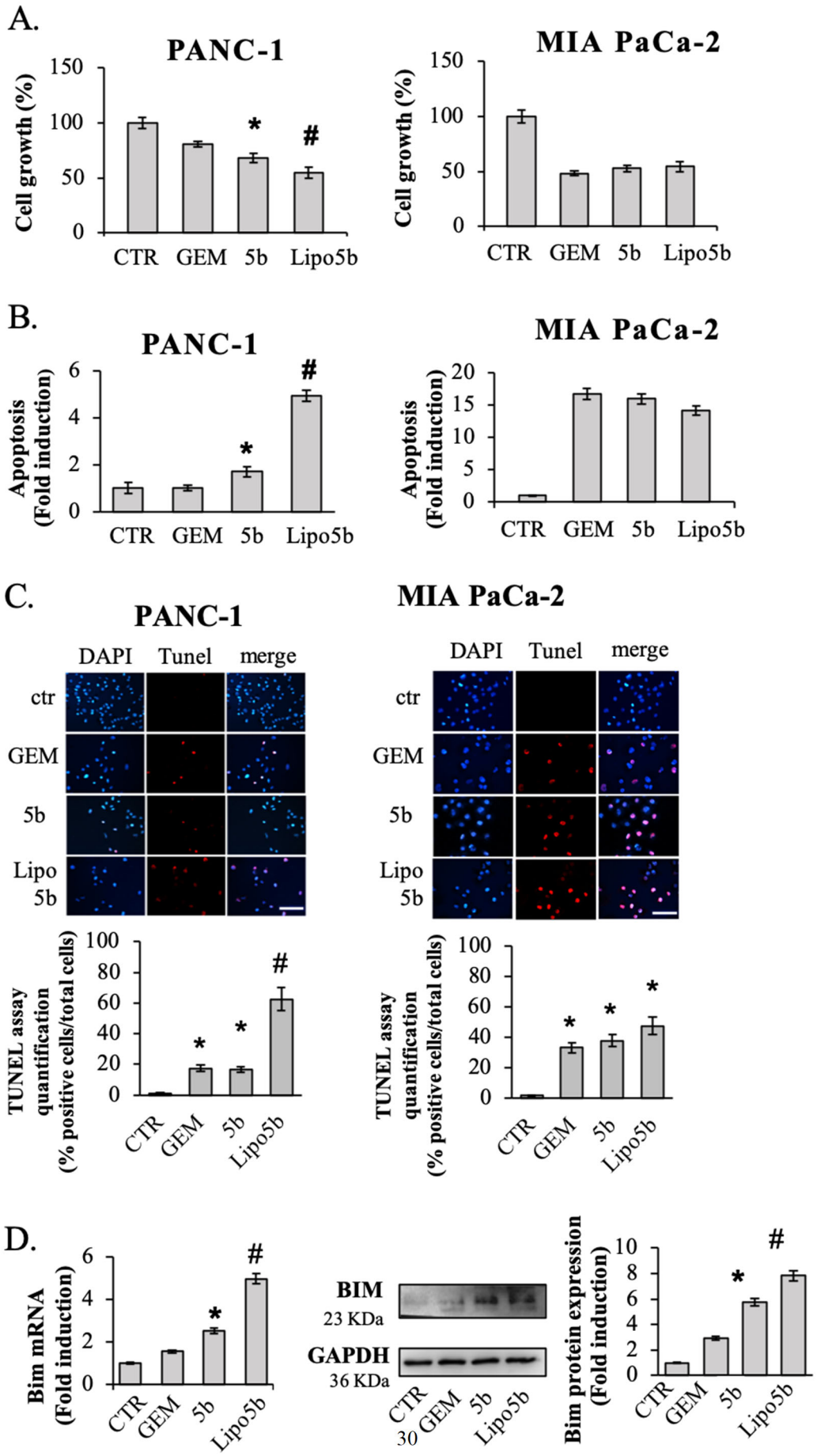
A.
PANC-1
Cell growth (%)
150
100
50
0
*
#
CTR GEM 5b Lipo5b
MIA PaCa-2
Cell growth (%)
150
100
50
0
CTR GEM 5b Lipo5b
B.
PANC-1
Apoptosis (Fold induction)
6
4
2
0
*
#
CTR GEM 5b Lipo5b
MIA PaCa-2
Apoptosis (Fold induction)
20
15
10
5
0
CTR GEM 5b Lipo5b
C.
PANC-1
DAPI Tunel merge
ctr
GEM
5b
Lipo 5b
TUNEL assay quantification (% positive cells/total cells)
100
80
60
40
20
0
*
*
#
CTR GEM 5b Lipo5b
MIA PaCa-2
DAPI Tunel merge
ctr
GEM
5b
Lipo 5b
TUNEL assay quantification (% positive cells/total cells)
100
80
60
40
20
0
*
*
*
CTR GEM 5b Lipo5b
D.
Bim mRNA (Fold induction)
6
4
2
0
*
#
CTR GEM 5b Lipo5b
BIM
23 KDa
GAPDH
36 KDa
CTR GEM 5b Lipo5b
30
Bim protein expression (Fold induction)
10
8
6
4
2
0
*
#
CTR GEM 5b Lipo5b

Figure 6. Encapsulation of the compound 5b in liposomes (Lipo 5b) enhances 5b-induced apoptotic cell death in PANC-1 cells. Cytotoxic effect (A) and apoptosis (B) in PANC-1 cells treated with 100 μM GEM, 5b or Lipo 5b for 48h. Measurements were performed in triplicate and data are presented as means ± SD (n = 3). Student's t-test: *p < 0.05 5b versus GEM; # p < 0.05 Lipo 5b versus 5b. C) Representative imagines of three similar experiments and quantification of TUNEL staining in PANC-1 and MIA PaCa-2 cells treated with 100 μM GEM, 5b or Lipo 5b for 48h. Student's t-test: *p < 0.05 GEM or 5b or Lipo 5b versus CTR; #p < 0.05 Lipo 5b versus 5b. D) qPCR and Western blot analysis of Bim expression in PANC-1 treated with 100 μM GEM, 5b or Lipo 5b for 48h. Student's t-test: *p < 0.05 5b versus GEM; #p < 0.05 Lipo 5b versus 5b.

The intracellular release of NO by 5b or Lipo 5b is determinant to increase their cytotoxic effect

To functionally investigate the role of NO released by **5b** and **Lipo 5b** on GEM-R PANC-1 cell growth inhibition, we first analyzed the effective enhancement of the intracellular NO level after cell treatment with GEM, **5b** or **Lipo 5b**, in the absence or presence of the NO scavenger PTIO or the nitric-oxide synthase (NOS) inhibitor L-NAME. **Figure 7A** shows that GEM treatment slightly increased the level of NO, which was completely reverted by L-NAME, in accordance with the previous observation that GEM triggered the NOS pathway in breast cancer cells[17]. Moreover, we demonstrated that **5b** and **Lipo 5b** further enhanced the intracellular NO level, which was strongly reverted by PTIO, suggesting that NO increase by **5b** or **5b** encapsulated in liposomes is mainly due to the intracellular release of NO by the pro-drug rather that determined by the endogenous NO production induced by NOS pathway stimulation. Functionally, we demonstrated that apoptosis (**figure 7B**) and cell growth inhibition (**figure 7C**) by **5b** and **Lipo 5b** is recovered by PTIO, indicating a role of NO released by the pro-drug on the acquisition of chemosensitivity to GEM in GEM-R PANC-1 cells.

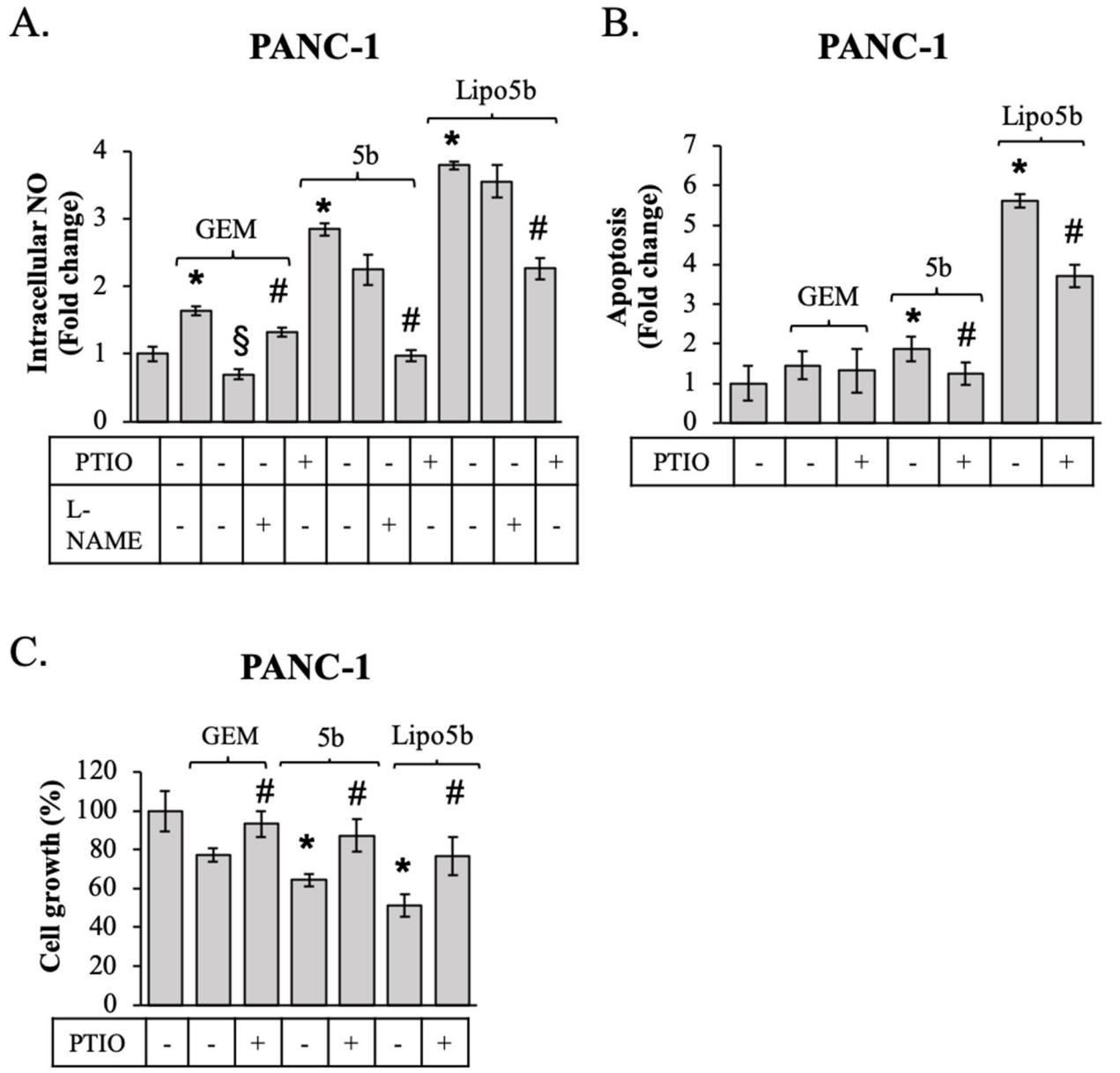

Figure 7. Detection of intracellular NO amount after GEM, 5b or Lipo 5b treatments and its role in cytotoxicity. PANC-1 cells were treated for 48h with GEM, 5b, Lipo 5b or PTIO 100 µM; L-NAME 1mM. Intracellular NO (A), apoptosis (B) and cell growth (C) were analyzed as reported in the Experimental Section. Measurements were performed in triplicate and data are presented as means ± SD (n = 3). Student's t-test: *p < 0.05 GEM, 5b or Lipo 5b versus CTR; §p < 0.05 GEM + L-NAME versus GEM; #p < 0.05 GEM, 5b or Lipo 5b + PTIO versus GEM, 5b or Lipo 5b, respectively.

MRP5 nitration by 5b or Lipo 5b confers chemosensitivity to GEM-R cells

Since it has been previously demonstrated that GEM can be a substrate of MRP5 pump, which favors the extracellular efflux of the drug reducing its citotoxic effects[5], and we previosly demonstrate that the nitration of MRP transporters impair their catalytic efficiency[18, 19, 20] we tested whether NO

released by **5b** pro-drug may nitrate the MRP5 pump affecting its activity. First, we analyzed the expression levels of MRP5 protein in a panel of six PDAC cell lines. Notably, **figures 8A** and **8B** show that MRP5 is more expressed in PDAC cell lines with higher IC_{50} value for GEM (PANC-1, PaCa3 and PaCa44), as compared to PDAC cell lines with lower IC_{50} value for GEM (MIAPaCa-2, T3M4, CFPAC), suggesting the involvement of MRP5 expression in GEM chemoresistance. Importantly, we also demonstrated by immunoblotting that treatments with **5b** nitrated the MRP5 pump in GEM-R PANC-1 cells, characterized by high expression levels of this protein. By contrast, we did not detect any nitration in GEM-S MIAPaCa-2 cells, except in the case of NO donor (**figure 8C**). Such different profile may be explained by the lower level of MRP5 in MIAPaCa-2 cells: in these conditions, only a strong NO releasing agent as SNAP[13] release sufficient amount of NO to produce a detectable nitration; the amount of NO released by **5b** likely induces a nitration rate that is below the detection limit of immunoblot. S-nitrosylation on cysteines was absent (not shown). Furthermore, we also observed a stronger MRP5 nitration in PANC-1 cells treated with **5b** encapsulated in liposomes, according to the increased uptake of the drug by liposomes delivery (figure 8C). This post-translational modification of the MRP5 pump is likely due to the intracellular release of NO by the pro-drug. We further investigated the impact of this post-translation modification on the activity of the MRP5 pump. **Figure 8D** shows that, in line with the different expression levels, the basal endogenous activity of MRP5 is higher in PANC-1 cells than in MIAPaCa-2 cells and that it is strongly inhibited after treatment with **5b** or **Lipo 5b** in GEM-R PANC-1 cells. In MIAPaCa-2 cells, on the other hand, the activity of the MRP5 pump is not affected by the pro-drug, in line with the absence of protein nitration. Finally, to demonstrate the role of MRP5 inhibition in the acquisition of sensitivity to GEM we knocked-down MRP5 expression by using 3 different shRNAs for MRP5, as shown in **supplementary figure 3**. MRP5 knock-down by shMRP5 #2 strongly enhanced the sensitivity of PANC-1 cells to GEM, **5b** or **Lipo 5b** (**figure 8E**). Data not shown indicate that similar data have been obtained using shMRP5 #1 and #3. Altogether these data

strongly suggest the involvement of NO-mediated nitration in the inhibitory effect of MRP5 activity and in the enhanced cytotoxic effect of **5b** pro-drug, as compared to the standard drug GEM, in chemoresistant PDAC cells. Finally, encapsulation of the pro-drug is a valuable approach to further enhance **5b** uptake and its anti-tumoral effects in PDAC cells.

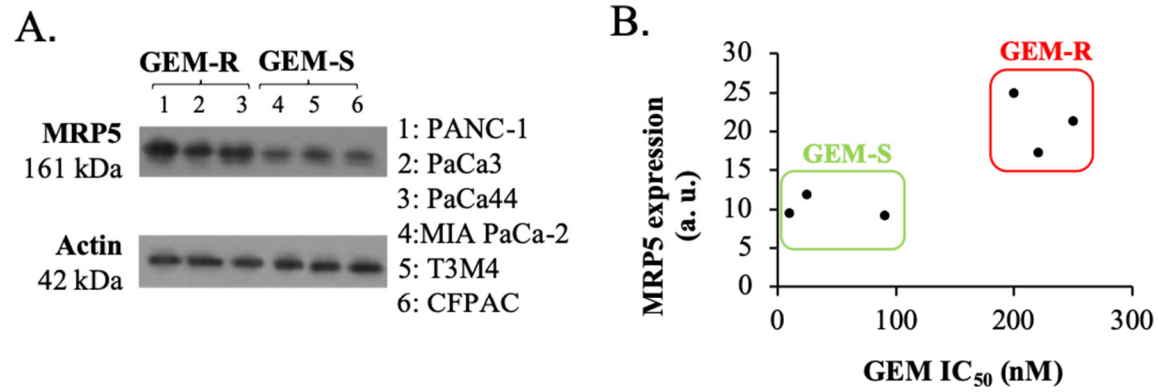
A.
GEM-R
GEM-S
1 2 3 4 5 6
MRP5
161 kDa
Actin
42 kDa
1: PANC-1
2: PaCa3
3: PaCa44
4:MIA PaCa-2
5: T3M4
6: CFPAC
B.
GEM-R
GEM-S
MRP5 expression (a. u.)
GEM IC50 (nM)
0
5
10
15
20
25
30
0
100
200
300

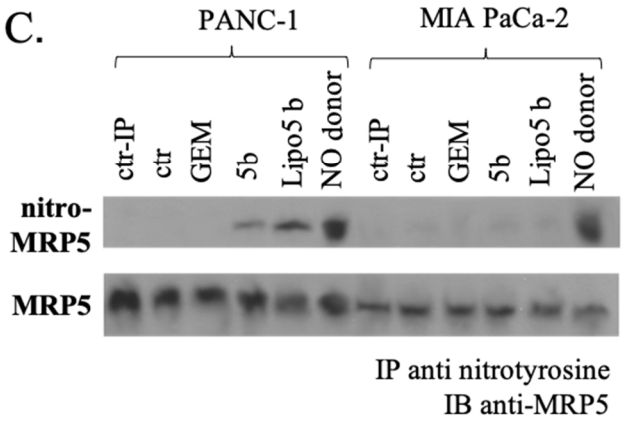
C.
PANC-1
MIA PaCa-2
ctr-IP
ctr
GEM
5b
Lipo5 b
NO donor
nitro-MRP5
MRP5
IP anti nitrotyrosine
IB anti-MRP5

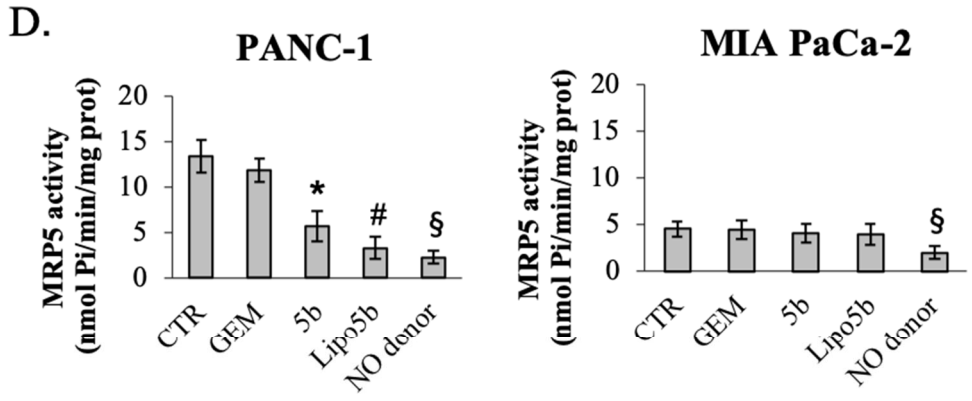
D.
PANC-1
MIA PaCa-2
MRP5 activity (nmol Pi/min/mg prot)
0
5
10
15
20
*
#
§
CTR
GEM
5b
Lipo5b
NO donor

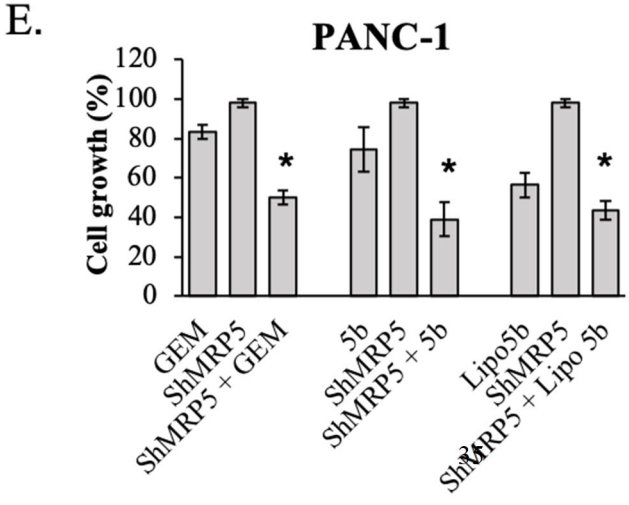
E.
PANC-1
Cell growth (%)
0
20
40
60
80
100
120
*
GEM
ShMRP5
ShMRP5 + GEM
5b
ShMRP5
ShMRP5 + 5b
Lipo5b
ShMRP5
ShMRP5 + Lipo 5b

Figure 8. MRP5 inhibition sensitizes PANC-1 cells to the treatment with GEM, 5b or Lipo 5b. A) Western Blotting analysis of MRP5 expression in GEM-R and GEM-S PDAC cell lines (A) and its relation with GEM IC_{50} values (B). Cells were treated with 100 μM GEM, 5b or Lipo 5b for 48h. NO donor: SNAP 100 μM. Cell protein extracts were used for MRP5 detection, nitration (C) and activity (D) as described in the Experimental Section. Student's t-test: *p <0.05 5b versus GEM; #p <0.05 Lipo 5b versus 5b; §p <0.05 NO donor versus CTR. (E) Cell growth analysis after MRP5 knock-down (by using shRNA#2) in the absence or presence of 100 μM GEM for 72h. Measurements were performed in triplicate and data are presented as means ± SD (n = 3). Student's t-test: *p <0.05 shMRP5 + GEM versus GEM; shMRP5 + 5b versus 5b; shMRP5 + Lipo 5b versus Lipo 5b.

DISCUSSION AND CONCLUSIONS

GEM is the standard chemotherapy used to treat PDAC since 1997. This drug is a cytidine analogue and its cytotoxic effect is mainly due to different mechanisms of nucleotide and DNA metabolism inhibition in cancer cells. However, although its wide use in clinic for its low toxic and side effects, it is not a completely effective and decisive treatment. GEM is indeed the target of many tumor-related molecular mechanisms of cancer cell resistance that can be innate or arise rapidly from the beginning of therapy. Most acquired resistance mechanisms mainly depend on the mutations developed by the tumor and its microenvironment, so the patients are differentially responsive to the therapy.[21,22]. In an effort to overcome GEM chemoresistance, several approaches are being developed including non-coding RNA, encapsulation in nanoparticles and liposomes, chemoresistance-related signaling pathway antagonists, immunotherapy, precise therapy based on molecular types.[23,24,25]. In a previous study, we have synthetized different gemcitabine lipophilic pro-drugs, that were efficiently loaded into liposomes unlike standard GEM that has proven to be difficult to encapsulate.[26] In particular, the [4-(*N*)-lauroyl-gemcitabine; C12GEM] derivative was further encapsulated in hyaluronic acid (HA)-decorated liposomes for cellular drug delivery, overcoming limitations due to the intracellular drug influx rate by nucleoside transporters and favoring drug delivery in CD44-overexpressing cancer cells[27,28].

In the present study, we designed and synthetized seven novel pro-drugs adding NO-donor moieties to GEM by an appropriate linker, in order to obtain different therapeutic advantages: *i*) to protect the pro-drug from the inactivation by deamination catalyzed by deoxycytidine deaminase that transforms cytidine in uracil[29], thus improving its metabolic stability; *ii*) to confer a more lipophilic feature to the pro-drug for its effective encapsulation in liposomes, which cannot occur with standard GEM; *iii*) to release NO into the cells. Indeed, the nitric moieties are organic nitrates (nitric esters) that release NO through enzymatic pathways and it has been reported that high intracellular concentrations of NO can produce anti-tumor effects shifting the balance towards cell death.[30] Thus,

NO is now considered a valuable molecule that can sensitize cancer cells to chemotherapy, as previously demonstrated for doxorubicin drug in colon cancer cells.[13] The best effect among the seven pro-drugs synthetized was obtained by **5b** and its effect is more evident in GEM-R PANC-1 cells, as also revealed by the combined treatment of GEM with the NO-donor diethylamine NONOate. In order to further enhance **5b** uptake into the cells, we encapsulated the pro-drug in liposomes, favoring drug delivery as revealed by the stronger intracellular accumulation of the drug after cell treatment with **Lipo 5b**, as compared to the non-encapsulated **5b** pro-drug. Intriguingly, **5b** and especially **Lipo 5b** enhanced the apoptosis level in GEM-R cells. These data were supported also by the increased expression level of the pro-apoptotic protein Bim in PANC-1 cells treated with **5b** or **Lipo 5b** compared with standard GEM treatment. Bim is a member of the Bcl-2 family that promotes apoptosis trough the mitochondrial intrinsic pathway [31] and whose expression is often suppressed in cancer cells, allowing tumor progression and metastasis[32].

No released by **5b** plays a fundamental role in decreasing cell growth and increasing apoptosis, in fact, by counteracting the intracellular NO increase with the NO scavenger PTIO, cell growth is recovered and concomitantly apoptosis stimulation is decreased. The effect of NO released into the cells was further studied by investigating the involvement of MRP5 tyrosine nitration, leading to its reduced activity and therefore to increased intracellular GEM concentration. Tyrosine nitration in biological systems can be promoted either by NO-dependent oxidative processes induced by NO release or by peroxynitrite-derived radicals, which is a short-lived and reactive biological oxidant formed from the reaction of the O_2•- and NO. Remarkably, mitochondrial superoxide ions production is a mechanism of action induced by GEM[33], thus it is conceivable that tyrosine nitration can be derived, at least partially, by $ONOO^-$ reaction produced by the intracellular NO released by the **5b** pro-drug in association to superoxide ions induced by GEM. In the case of MRP proteins, a nitration on tyrosine is commonly associated to a reduction of the catalytic efficiency of the transporters[18, 19, 20]. Interestingly, the MRP5 pump confers resistance to the treatment of the cells with GEM[15] and it

is more expressed in GEM-R, as compared to GEM-S PDAC cell lines. Our data suggest that MRP5 pump is nitrated and inhibited by NO released by **5b** and especially by **Lipo 5b**. This stable post-translational modification is paralleled by a decrease in the ATPase activity of MRP5 that results in a decreased efflux of GEM. The increased intracellular accumulation of GEM thus enhanced its anti-tumoral effects. We cannot exclude that S-nitrosylation also occur, but we did not detect in our conditions, likely because of the transient nature of S-nitrosylation that is a more labile modification that tyrosine nitration[34] or because of the simultaneous release of O_2•- and NO from **5b**, a condition leading to the increase of intracellular $ONOO^-$, a strong tyrosine-nitrating species[9] and a cytotoxic radical[35]. Overall data shown in the present study can provide a preclinical evaluation of the possible usage of NO-GEM pro-drugs encapsulated in liposomes for the treatment of chemoresistant PDAC patients. Further investigations will be addressed to functionalize liposomes with novel and attractive cancer-related ligands for tumor-specific drug delivery and to test their effect in *in vivo* cancer models.

ACKNOWLEDGMENTS

This work was supported by Italian Ministry of Education, University and Research (MIUR); by Joint Project (call 2017) from the University of Verona (n. B33C17000030003); by "Associazione Italiana Ricerca sul Cancro" (AIRC) (n. IG 21408). We also acknowledge the "Technological Platforms Center" (CPT) of the University of Verona for the biotechnological support to this study and "Ricerca Locale" from the University of Turin for financial support. This work was also supported by a project funded by the CariVerona Foundation with a PhD fellowship to Dr. Francesca Masetto at the University of Verona.

CONFLICT OF INTEREST

All authors declare that they have no conflicts of interest.

REFERENCES

1. Siegel, R. L., Miller, K. D. & Jemal, A. Cancer Statistics , 2018. **68**, 7–30 (2018).

2. American Cancer Society. Cancer Facts. *Cancer Facts* 1–9 (2016). doi:10.1097/01.NNR.0000289503.22414.79

3. Young, J. D., Yao, S. Y. M., Sun, L., Cass, C. E. & Baldwin, S. A. Human equilibrative nucleoside transporter (ENT) family of nucleoside and nucleobase transporter proteins. *Xenobiotica* (2008). doi:10.1080/00498250801927427

4. Amrutkar, M. & Gladhaug, I. P. Pancreatic cancer chemoresistance to gemcitabine. *Cancers* (2017). doi:10.3390/cancers9110157

5. Kohan, H. G. & Boroujerdi, M. Time and concentration dependency of P-gp, MRP1 and MRP5 induction in response to gemcitabine uptake in Capan-2 pancreatic cancer cells. *Xenobiotica* (2015). doi:10.3109/00498254.2014.1001809

6. Cho, J. H., Kim, S. A., Park, S. B., Kim, H. M. & Song, S. Y. Suppression of pancreatic adenocarcinoma upregulated factor (PAUF) increases the sensitivity of pancreatic cancer to gemcitabine and 5FU, and inhibits the formation of pancreatic cancer stem like cells. *Oncotarget* (2017). doi:10.18632/oncotarget.19458

7. Zeng, S. *et al.* Chemoresistance in pancreatic cancer. *International Journal of Molecular Sciences* (2019). doi:10.3390/ijms20184504

8. König, J. *et al.* Expression and localization of human multidrug resistance protein (ABCC) family members in pancreatic carcinoma. *Int. J. Cancer* (2005). doi:10.1002/ijc.20831

9. Ignarro, L. J. *Nitric Oxide: Biology and Pathobiology*. *The effects of brief mindfulness*

intervention on acute pain experience: An examination of individual difference (2009). doi:10.1017/CBO9781107415324.004

10. Seth, D. *et al.* A Multiplex Enzymatic Machinery for Cellular Protein S-nitrosylation. *Mol. Cell* (2018). doi:10.1016/j.molcel.2017.12.025

11. Bartesaghi, S. & Radi, R. Fundamentals on the biochemistry of peroxynitrite and protein tyrosine nitration. *Redox Biology* (2018). doi:10.1016/j.redox.2017.09.009

12. Zhan, X., Huang, Y. & Qian, S. Protein Tyrosine Nitration in Lung Cancer: Current Research Status and Future Perspectives. *Curr. Med. Chem.* (2018). doi:10.2174/0929867325666180221140745

13. Riganti, C. *et al.* Nitric oxide reverts the resistance to doxorubicin in human colon cancer cells by inhibiting the drug efflux. *Cancer Res.* (2005). doi:65/2/516 [pii]

14. Donadelli, M. *et al.* Synergistic inhibition of pancreatic adenocarcinoma cell growth by trichostatin A and gemcitabine. *Biochim. Biophys. Acta - Mol. Cell Res.* **1773**, 1095–1106 (2007).

15. Hagmann, W., Jesnowski, R. & Löhr, J. M. Interdependence of gemcitabine treatment, transporter expression, and resistance in human pancreatic carcinoma cells. *Neoplasia* (2010). doi:10.1593/neo.10576

16. Guo, Z. W. & Gallo, J. M. Selective protection of 2',2'-difluorodeoxycytidine (gemcitabine). *J. Org. Chem.* (1999). doi:10.1021/jo9911140

17. Zeybek, N. D. *et al.* The effects of Gemcitabine and Vinorelbine on inducible nitric oxide synthase (iNOS) and endothelial nitric oxide synthase (eNOS) distribution of MCF-7 breast

cancer cells. *Acta Histochem.* (2011). doi:10.1016/j.acthis.2009.07.006

18. De Boo, S. *et al.* INOS activity is necessary for the cytotoxic and immunogenic effects of doxorubicin in human colon cancer cells. *Mol. Cancer* (2009). doi:10.1186/1476-4598-8-108

19. Pedrini, I. *et al.* Liposomal nitrooxy-doxorubicin: One step over Caelyx in drug-resistant human cancer cells. *Mol. Pharm.* (2014). doi:10.1021/mp500257s

20. Di Pietro, N. *et al.* Nitric oxide synthetic pathway and cGMP levels are altered in red blood cells from end-stage renal disease patients. *Mol. Cell. Biochem.* (2016). doi:10.1007/s11010-016-2723-0

21. Pan, S. T., Li, Z. L., He, Z. X., Qiu, J. X. & Zhou, S. F. Molecular mechanisms for tumour resistance to chemotherapy. *Clinical and Experimental Pharmacology and Physiology* **43**, 723–737 (2016).

22. Fiorini, C. *et al.* Mutant p53 stimulates chemoresistance of pancreatic adenocarcinoma cells to gemcitabine. *Biochim. Biophys. Acta - Mol. Cell Res.* (2015). doi:10.1016/j.bbamcr.2014.10.003

23. Luo, W. *et al.* Novel discoveries targeting gemcitabine-based chemoresistance and new therapies in pancreatic cancer: How far are we from the destination? *Cancer Med.* (2019). doi:10.1002/cam4.2384

24. Dalla Pozza, E. *et al.* Gemcitabine response in pancreatic adenocarcinoma cells is synergistically enhanced by dithiocarbamate derivatives. *Free Radic. Biol. Med.* (2011). doi:10.1016/j.freeradbiomed.2011.01.001

25. Fiorini, C., Cordani, M., Gotte, G., Picone, D. & Donadelli, M. Onconase induces autophagy

sensitizing pancreatic cancer cells to gemcitabine and activates Akt/mTOR pathway in a ROS-dependent manner. *Biochim. Biophys. Acta - Mol. Cell Res.* **1853**, 549–560 (2015).

26. Immordino, M. L. *et al.* Preparation, characterization, cytotoxicity and pharmacokinetics of liposomes containing lipophilic gemcitabine prodrugs. *J. Control. Release* (2004). doi:10.1016/j.jconrel.2004.09.001

27. Arpicco, S. *et al.* Hyaluronic acid-coated liposomes for active targeting of gemcitabine. *Eur. J. Pharm. Biopharm.* **85**, 373–380 (2013).

28. Dalla Pozza, E. *et al.* Targeting gemcitabine containing liposomes to CD44 expressing pancreatic adenocarcinoma cells causes an increase in the antitumoral activity. *Biochim. Biophys. Acta - Biomembr.* **1828**, 1396–1404 (2013).

29. Arpicco, S. *et al.* Recent studies on the delivery of hydrophilic drugs in nanoparticulate systems. *Journal of Drug Delivery Science and Technology* (2016). doi:10.1016/j.jddst.2015.09.004

30. Huang, Z., Fu, J. & Zhang, Y. Nitric Oxide Donor-Based Cancer Therapy: Advances and Prospects. *Journal of Medicinal Chemistry* (2017). doi:10.1021/acs.jmedchem.6b01672

31. O'Connor, L. *et al.* Bim: A novel member of the Bcl-2 family that promotes apoptosis. *EMBO J.* (1998). doi:10.1093/emboj/17.2.384

32. Sionov, R. V., Vlahopoulos, S. A. & Granot, Z. Regulation of Bim in Health and Disease. *Oncotarget* (2015). doi:10.18632/oncotarget.5492

33. Dalla Pozza, E. *et al.* Role of mitochondrial uncoupling protein 2 in cancer cell resistance to gemcitabine. *Biochim. Biophys. Acta - Mol. Cell Res.* (2012).

doi:10.1016/j.bbamcr.2012.06.007

34. Anand, P. & Stamler, J. S. Enzymatic mechanisms regulating protein s-nitrosylation: Implications in health and disease. *Journal of Molecular Medicine* (2012). doi:10.1007/s00109-012-0878-z

35. Radi, R. Peroxynitrite, a stealthy biological oxidant. *Journal of Biological Chemistry* (2013). doi:10.1074/jbc.R113.472936

36. Kartasasmita, R. E., Laufer, S. & Lehmann, J. NO-donors (VII [1]): Synthesis and cyclooxygenase inhibitory properties of N- and S-nitrooxypivaloyl-cysteine derivatives of naproxen - A novel type of NO-NSAID. *Arch. Pharm. (Weinheim).* (2002). doi:10.1002/1521-4184(200211)335:8<363::AID-ARDP363>3.0.CO;2-S

37. Lazzarato, L. *et al.* (Nitrooxyacyloxy)methyl esters of aspirin as novel nitric oxide releasing aspirins. *J. Med. Chem.* (2009). doi:10.1021/jm900587h

38. BARTLETT, G. R. Phosphorus assay in column chromatography. *J. Biol. Chem.* (1959).

39. Freyria, F. S. *et al.* Hematite nanoparticles larger than 90 nm show no sign of toxicity in terms of lactate dehydrogenase release, nitric oxide generation, apoptosis, and comet assay in murine alveolar macrophages and human lung epithelial cells. *Chem. Res. Toxicol.* (2012). doi:10.1021/tx2004294

40. Chegaev, K. *et al.* Light-Regulated NO Release as a Novel Strategy To Overcome Doxorubicin Multidrug Resistance. *ACS Med. Chem. Lett.* **8**, 361–365 (2017).

Table of Contents graphic (TOC)